



RACK1 Associates with RNA-Binding Proteins Vigilin and SERBP1 to Facilitate Dengue Virus Replication

Alexis Brugier,^a Mohamed Lamine Hafirassou,^a Marie Pourcelot,^a Morgane Baldaccini,^b Vasiliya Kril,^a Laurine Couture,^a Beate M. Kümmerer,^c Sarah Gallois-Montbrun,^d Lucie Bonnet-Madin,^a Pierre-Olivier Vidalain,^e Constance Delaugerre,^{a,f} Sébastien Pfeffer,^b Laurent Meertens,^a Ali Amara^a

^aUniversité de Paris, INSERM U944, CNRS 7212, Biology of Emerging Viruses Team, Institut de Recherche Saint-Louis, Hôpital Saint-Louis, Paris, France

^bUniversité de Strasbourg, Architecture et Réactivité de l'ARN, Institut de Biologie Moléculaire et Cellulaire du CNRS, Strasbourg, France

^cInstitute of Virology, Medical Faculty, University of Bonn, Bonn, Germany

^dUniversité de Paris, Institut Cochin, INSERM U1016, CNRS UMR8104, Paris, France

^eCentre International de Recherche en Infectiologie, Team Viral Infection, Metabolism and Immunity, INSERM U1111, CNRS UMR5308, ENS de Lyon, Université Claude Bernard Lyon 1, Lyon, France

^fLaboratoire de Virologie et Département des Maladies Infectieuses, Hôpital Saint-Louis, Assistance Publique–Hôpitaux de Paris, Paris, France

Alexis Brugier and Mohamed Lamine Hafirassou contributed equally to this article. Author order was determined by the corresponding author after negotiation.

ABSTRACT Dengue virus (DENV) is a mosquito-borne flavivirus responsible for dengue disease, a major human health concern for which no effective treatment is available. DENV relies heavily on the host cellular machinery for productive infection. Here, we show that the scaffold protein RACK1, which is part of the DENV replication complex, mediates infection by binding to the 40S ribosomal subunit. Mass spectrometry analysis of RACK1 partners coupled to an RNA interference screen-identified Vigilin and SERBP1 as DENV host-dependency factors. Both are RNA-binding proteins that interact with the DENV genome. Genetic ablation of Vigilin or SERBP1 rendered cells poorly susceptible to DENV, as well as related flaviviruses, by hampering the translation and replication steps. Finally, we established that a Vigilin or SERBP1 mutant lacking RACK1 binding but still interacting with the viral RNA is unable to mediate DENV infection. We propose that RACK1 recruits Vigilin and SERBP1, linking the DENV genome to the translation machinery for efficient infection.

IMPORTANCE We recently identified the scaffolding RACK1 protein as an important host-dependency factor for dengue virus (DENV), a positive-stranded RNA virus responsible for the most prevalent mosquito-borne viral disease worldwide. Here, we have performed the first RACK1 interactome in human cells and identified Vigilin and SERBP1 as DENV host-dependency factors. Both are RNA-binding proteins that interact with the DENV RNA to regulate viral replication. Importantly, Vigilin and SERBP1 interact with RACK1 and the DENV viral RNA (vRNA) to mediate viral replication. Overall, our results suggest that RACK1 acts as a binding platform at the surface of the 40S ribosomal subunit to recruit Vigilin and SERBP1, which may therefore function as linkers between the viral RNA and the translation machinery to facilitate infection.

KEYWORDS dengue virus, host factors, RACK1, RNA-binding proteins, SERBP1, Vigilin

Dengue virus (DENV) belongs to the genus *Flavivirus* of the family *Flaviviridae*, which includes important emerging and reemerging viruses such as West Nile virus (WNV), yellow fever virus (YFV), Zika virus (ZIKV), and tick-borne encephalitis virus (TBEV) (1). DENV is transmitted to humans by an *Aedes* mosquito bite and may lead to a variety of diseases ranging from mild fever to lethal dengue hemorrhagic fever and dengue shock syndrome (2). Recent estimations indicate that half of the world's

Editor Anice C. Lowen, Emory University School of Medicine

Copyright © 2022 American Society for Microbiology. All Rights Reserved.

Address correspondence to Ali Amara, ali.amara@inserm.fr.

The authors declare no conflict of interest.

Received 16 November 2021

Accepted 24 January 2022

Published 10 March 2022

population lives in areas where dengue fever is endemic (3), with 100 million symptomatic infections, including 500,000 cases of severe manifestations of the disease per year (4). There are currently no approved antiviral therapies against DENV, although a promising inhibitor targeting the viral NS3-NS4B interaction was recently described (5). Conversely, the recently approved tetravalent live attenuated vaccine showed disappointing efficacy (6, 7).

DENV is an enveloped virus containing a positive-stranded RNA genome of ~11 kb. Upon entry into the host cell, the viral genome is released in the cytoplasm and translated by the host machinery into a large polyprotein precursor that is processed by host and viral proteases. Co- and posttranslational processing gives rise to three structural proteins: the C (core), prM (precursor of the M protein), and E (envelope) glycoproteins, which form the viral particle and seven nonstructural proteins (NS) called NS1, NS2A, NS2B, NS3, NS4A, NS4B, and NS5 (8) that play central roles in viral genome replication, assembly, and modulation of innate immune responses (9). Like other flaviviruses, DENV genome replication takes place within virus-induced vesicles (Ve) derived from invaginations of the endoplasmic reticulum (ER) membrane (10, 11). These structures consist of 90-nm-wide vesicles containing a ± 11 -nm pore that allows exchanges between the Ve lumen and the cytosol (11). Within the Ve, viral NS proteins, viral RNA (vRNA), and some host factors assemble to form the viral replication complex (RC) that is essential for viral RNA synthesis. We have recently purified the DENV RC in human cells, using a tagged DENV subgenomic replicon, and determined its composition by mass spectrometry (12). Our study provided an unprecedented mapping of the DENV RC host interactome and identified cellular modules exploited by DENV during active replication. By combining these proteomics data with gene silencing experiments, we identified a set of host-dependency factors (HDFs) that have a critical impact on DENV infection and established an important role for RACK1 (receptor for activated C kinase 1) in DENV vRNA amplification (12), which was recently confirmed by others (13).

RACK1 is a core component of the 40S ribosomal subunit (14, 15), containing seven WD40 domains that mediate protein-protein interactions (16, 17). RACK1 is a scaffold protein (18, 19) described to interact with many cellular pathways such as Sarcoma (Src) tyrosine kinase (20, 21), cAMP/protein kinase A (PKA) (22), or receptor tyrosine kinase (23). Ribosomal RACK1 has also been shown to be involved in the association of mRNAs with polysomes (24), in the recruitment and phosphorylation of translational initiation factors (25–27), and in quality control during translation (28). The nonribosomal form of RACK1 is involved in innate immunity, by recruiting the PP2A phosphatase (29) or by targeting the VISA/TRAF complexes (30), and participates in the assembly and activation of the NLRP3 inflammasome (31). To date, only one proteomic study aiming to identify RACK1 cofactors has been performed in *Drosophila* S2 cells (32). RACK1 cellular partners in human cells are largely unknown.

Several viruses depend on RACK1 to complete their infectious cycle^{31–35}. For instance, RACK1 is involved in internal ribosome entry site (IRES)-mediated translation of viruses possessing a type I IRES such as cricket paralysis virus or hepatitis C virus (33). RACK1 also contributes to poxvirus infection through a ribosome customization mechanism. Indeed, poxviruses trigger the phosphorylation of the serine 278 of RACK1 (34) to promote the selective translation of viral RNAs.

In this work, we have investigated the function of RACK1 during DENV life cycle. We performed the first interactome of RACK1 in human cells. Functional studies revealed that RACK1 interacts with the RNA-binding proteins Vigilin and SERBP1 to facilitate DENV replication.

RESULTS AND DISCUSSION

RACK1 interaction with the 40S ribosomal subunit is required for DENV infection.

To confirm the role of RACK1 in DENV infection, we challenged parental and RACK1 knockout (RACK1^{KO}) HAP1 cells with DENV2-16681 particles at different multiplicities of infection (MOIs) and measured viral infection by quantifying the percentage of cells

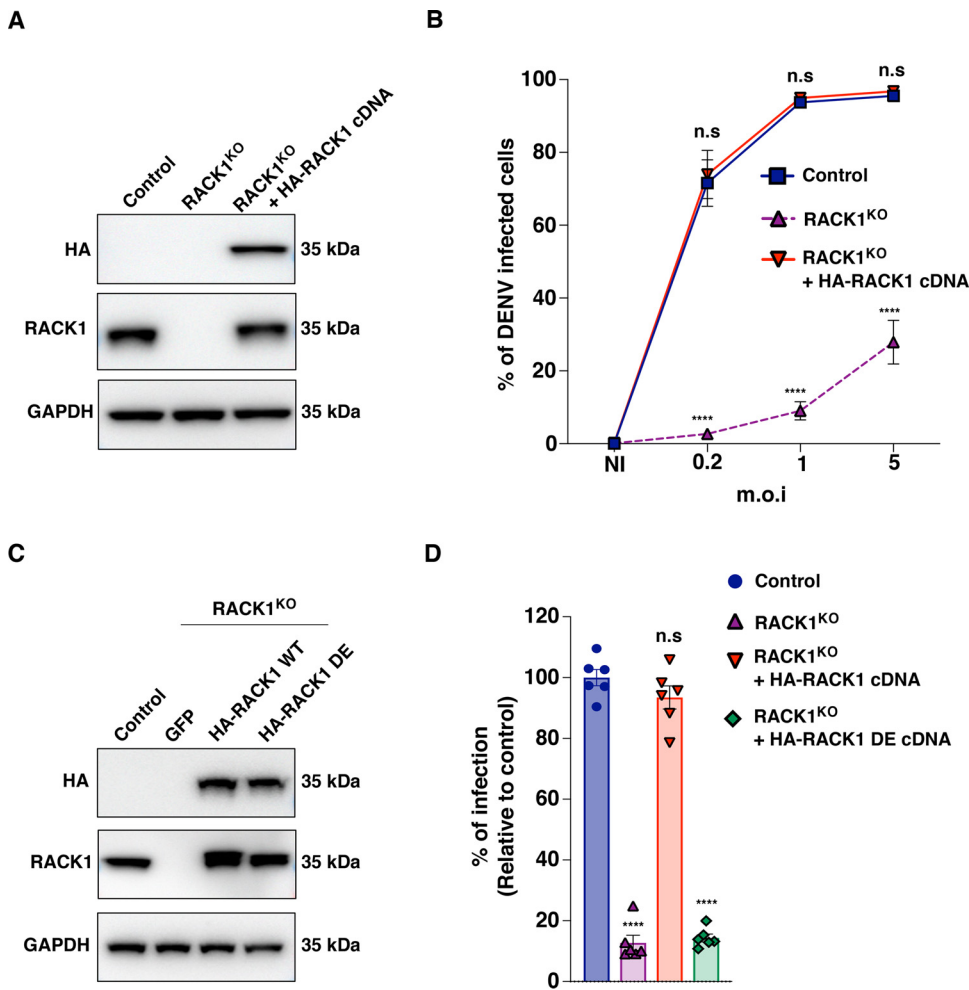


FIG 1 The interaction between RACK1 and the 40S ribosome is required for dengue virus (DENV) infection. (A) Western blot analysis of RACK1 expression in control, RACK1^{KO}, and RACK1^{KO} HAP1 cells transcomplemented with a hemagglutinin (HA)-RACK1 cDNA. Cell lysates were probed with the indicated antibodies. Shown is a representative Western blot of *n* = 3 technically independent experiments. (B) Role of RACK1 in DENV infection. Control, RACK1^{KO}, or RACK1^{KO} cells transcomplemented with a cDNA encoding wild-type (WT) HA-RACK1 were infected at different multiplicities of infection (m.o.i) with DENV2-16681. Levels of infection were determined by flow cytometry using the 2H2 prM monoclonal antibody (Mab) at 48 h postinfection (hpi). The data shown are the means ± standard error of the mean (SEM) of four independent experiments performed in duplicate. Significance was calculated using two-way analysis of variance (ANOVA) with Dunnett's multiple-comparison test. (C) Western blot analysis of RACK1 expression in RACK1^{KO} HAP1 transcomplemented with cDNA encoding WT HA-RACK1 or the HA-RACK1 D/E mutant (HA-RACK1 DE cDNA). Cell lysates were probed with the indicated antibodies. Shown is a representative Western blot of three independent experiments. (D) Impact of RACK1 association to the 40S subunit of the ribosome in DENV infection. Control, RACK1^{KO}, and RACK1^{KO} HAP1 cells transcomplemented with cDNA encoding WT HA-RACK1 or the HA-RACK1 DE mutant were infected at MOI 1 with DENV2-16681 and harvested at 48 hpi. Levels of infection were determined by flow cytometry as described above. The data shown are the means ± SEM of three independent experiments performed in duplicate. Significance was calculated using one-way ANOVA with Dunnett's multiple-comparison test. ****, *P* < 0.0001; n.s., not significant; GAPDH, glyceraldehyde-3-phosphate dehydrogenase; GFP, green fluorescent protein; NI, not infected.

expressing the DENV antigen PrM. In agreement with our previous studies (12), DENV infection was severely impaired in HAP1 cells lacking RACK1 (Fig. 1A and B). Importantly, transcomplementation of the HAP1 RACK1^{KO} cells with a plasmid encoding human RACK1 rescued cell susceptibility to DENV infection (Fig. 1A and B), ruling out CRISPR-Cas9-mediated off-target effects and demonstrating that RACK1 is an important host factor for DENV.

RACK1 is a component of the 40S subunit of the ribosome and is located near the mRNA exit channel (17). To test whether DENV infection requires RACK1 association

with the 40S ribosome, we transcomplemented RACK1^{KO} cells with a RACK1 mutant defective for ribosome-binding (RACK1R36D/K38E, DE mutant) (34, 35). The RACK1 DE mutant, which displayed a wild-type (WT) expression level and was unable to associate with polysomes (data not shown and Ref. 36), failed to rescue DENV2-16681 infection (Fig. 1C and D). These results indicate that the interaction with the 40S ribosomal subunit is important for RACK1 proviral function.

Mapping the RACK1 interactome. Because RACK1 is a scaffold protein, we hypothesized that its proviral activity may rely on its ability to recruit host proteins near the ribosome for optimal translation. To characterize the RACK1 interactome in mammalian cells, we transfected 293T cells with a plasmid encoding an hemagglutinin (HA)-tagged version of human RACK1. We pulled down RACK1 and its binding partners using HA beads and eluted purified proteins with HA peptide according to the experimental procedures that we recently described (12). Immunoprecipitated proteins were separated by SDS-PAGE, visualized by silver staining, and subjected to mass spectrometry (MS) analysis (Fig. 2A). By analyzing the raw affinity purification-mass spectrometry (AP-MS) data set with SAINT express and MiST softwares (37), we identified 135 high-confidence host factors that copurified with RACK1 and showed a SAINT express score greater than 0.8 (supplemental material). Next, we analyzed the list of 135 high-confidence interactors with DAVID 6.8 to identify statistical enrichments for specific Gene Ontology (GO) terms from the “cellular component” (CC) annotation (38, 39) (Fig. 2B) and built the corresponding interaction network using Cytoscape 3.4.0 (40) (Fig. 2C). The 135 RACK1-interacting proteins were clustered into functional modules using enriched GO terms as a guideline and literature mining (Fig. 2C). As expected, the RACK1 interactome was significantly enriched in proteins associated with ribosome/polysome and mRNA translation (Rps3, eIF3, eIF4G, and eIF4J), stress granules (G3BP2 and LARP1), P-Bodies (Ago1 and 2), and RNA splicing factors (HNRNPA2B1 and U2AF2) (Fig. 2C). Interestingly, several proteins found in our study, such as Ago2, LARP1 and 2, and eIF3A, were also identified in a RACK1 interactome done in *Drosophila* S2 cells (32).

Vigilin, SERBP1, and ZNF598 are DENV host-dependency factors. To pinpoint the function of the RACK1 binding partners during DENV infection, we silenced by RNA interference (RNAi) the expression of the 49 highest ranked hits with an average peptide count of more than 28 and determined the consequences on viral infection (Fig. 3A; supplemental material). Four proteins, namely HNRNPA2B1, Vigilin, SERBP1, and ZNF598, whose silencing decreased infection by at least 50% without affecting cell viability in the two cell lines were considered for further investigation (Fig. 3A; supplemental material). These factors are RNA-binding proteins (RBP) involved in RNA splicing (HNRNPA2B1) (41) or translation regulation (Vigilin, SERBP1, and ZNF598) (28, 42, 43). HNRNPA2B1 was already described to interact with the 3'-untranslated region (UTR) part of the virus (44). Because HNRNPA2B1 is a nuclear protein (45), it was not further considered in our study. Vigilin is a multiple K-homology (KH) domain protein implicated in translation regulation and lipidic metabolism (24, 43, 46). This protein was recently described to bind the DENV RNA and, in association with the ribosomal-binding protein 1 (RRBP1), to facilitate viral RNA translation and replication (47). However, how this protein interacts with RACK1 to regulate DENV infection is still unknown. SERBP1 is a RACK1 cofactor (48) that is located at the entry channel of ribosomes (49) and enhances translation by promoting the association of mRNAs with polysomes (42). SERBP1 was also described to interact with DENV RNA. However, its role in DENV replication remains unclear (50). Finally, ZNF598 is an E3 ubiquitin-protein ligase known to interact with RACK1 and playing a key role in the ribosome quality control (28). ZNF598 was also described to play a role in innate immunity (51). However, its role in DENV infection is unknown.

We first confirmed that endogenous Vigilin, ZNF598, and SERBP1 proteins coimmunoprecipitated with HA-RACK1 ectopically expressed in 293T cells (Fig. 3B). Next, we validated the requirement of Vigilin, SERBP1, and ZNF598 using two approaches. On one hand, we found that knocking down by RNA interference Vigilin, SERBP1, or ZNF598 (Fig. 3C) significantly impaired DENV infection but not viability of primary human fibroblasts, which are DENV target cells (Fig. 3D and E). On the other hand, we

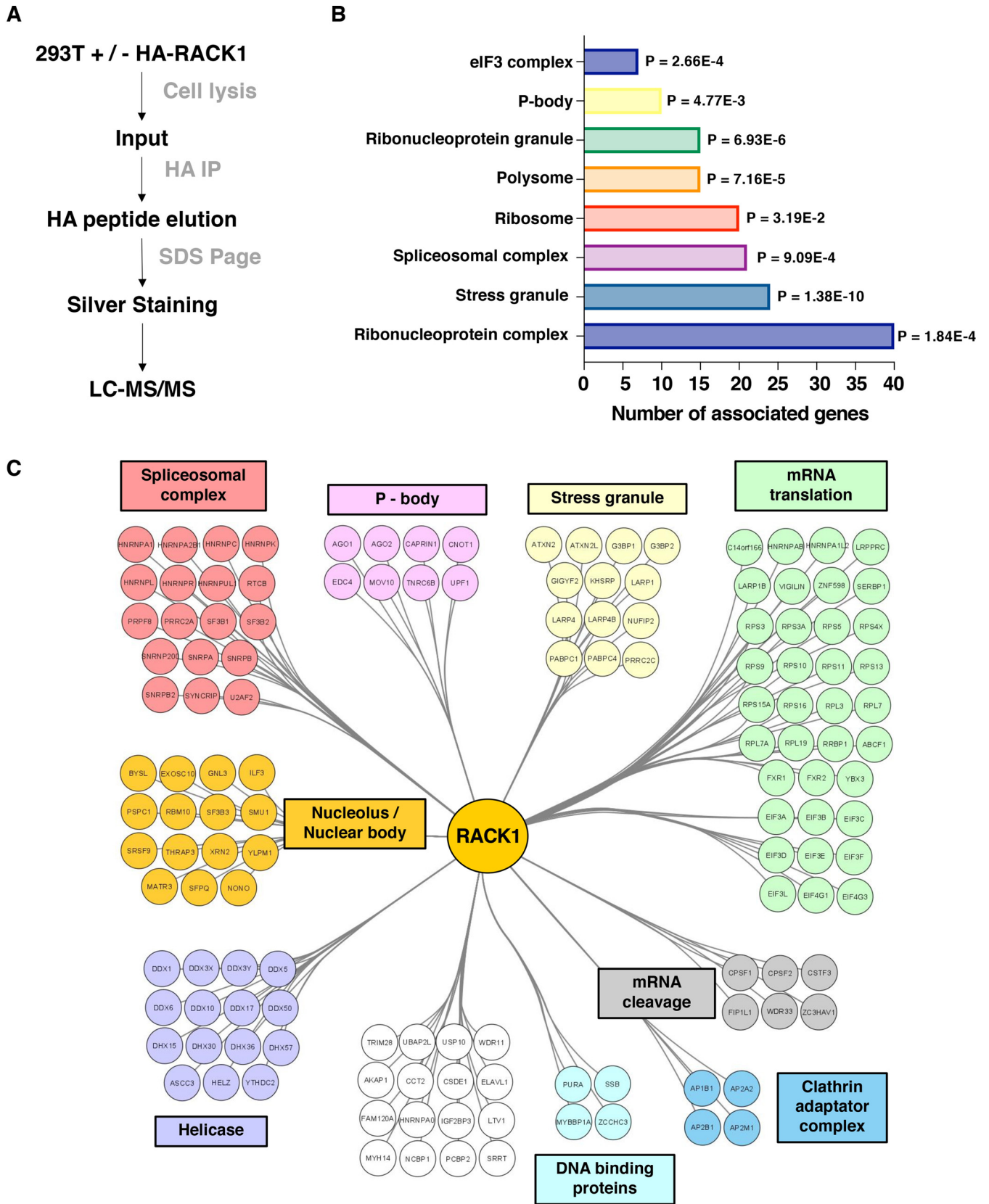


FIG 2 Global map of the RACK1 interactome in human cells. (A) Experimental scheme of our RACK1 immunoprecipitation approach. 293T cells expressing RACK1 or HA-RACK1 were lysed, and extracts were purified with anti-HA-coated beads before SDS-PAGE and mass spectrometry (MS) analysis. (B) Histogram indicating statistical enrichment for specific biological processes and cellular components, determined by Gene Ontology (GO) analysis.

(Continued on next page)

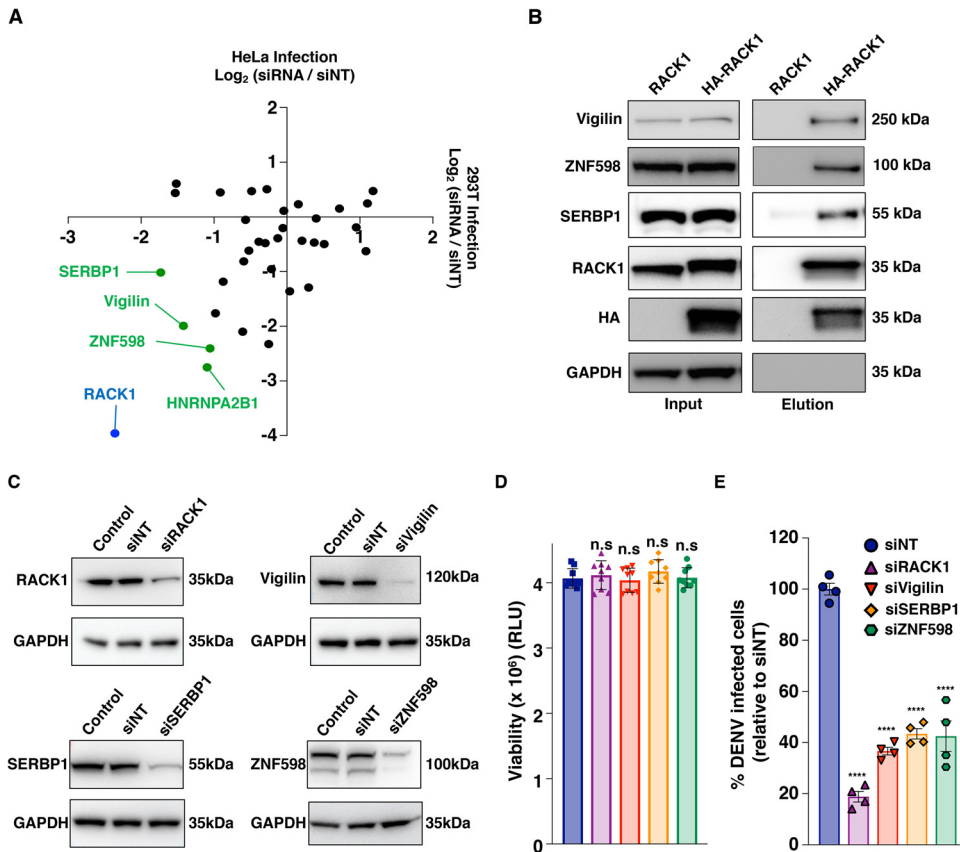


FIG 3 RNA interference (RNAi) screen-identified Vigilin, SERBP1, and ZNF598 are DENV host-dependency factors. (A) Host-dependency factors (HDFs) found in our RNAi screen. The data shown are representative of three independent experiments. Host-dependency factors are marked in green. The positive control (small interfering RNA [siRNA] pool targeting RACK1) is highlighted in blue. (B) Validation of the interaction between RACK1 and endogenous Vigilin or SERBP1 in 293T cells by immunoprecipitation. Cell extracts from 293T cells expressing RACK1 or HA-RACK1 were subjected to affinity purification using anti-HA beads, and interacting proteins were revealed by Western blotting. The data shown are representative of three independent experiments. (C) Human primary fibroblasts were transfected with the indicated siRNA pools. RACK1, Vigilin, SERBP1, and ZNF598 expression in siRNA transfected cells was assessed by Western blot analysis 48 h posttransfection. (D) The viability of siRNA transfected fibroblasts described in B was monitored by cell titer glow analysis. The data shown are the means ± SEM of three independent experiments performed in triplicate. Significance was calculated using two-way ANOVA with Dunnett’s multiple-comparison test. (E) siRNA transfected fibroblasts described for panel B were challenged with DENV2-16681 at MOI 1. At 48 h posttransfection, the levels of infection were determined by flow cytometry using 2H2 MAb at 48 hpi. The data shown are the means ± SEM of three independent experiments performed in duplicate. Significance was calculated using one-way ANOVA with Dunnett’s multiple-comparison test. RLU, relative light units; siNT, nontargeting siRNA.

used the CRISPR-Cas9 technology to edit the corresponding genes in HAP1 cells (Vigilin^{KO}, SERBP1^{KO}, and ZNF598^{KO}) (Fig. 4). Gene editing and knockout generation were confirmed by genomic DNA sequencing (Fig. 4A) and Western blot analysis (Fig. 4B), respectively. In agreement with our previous findings, lack of RACK1, Vigilin, SERBP1, and ZNF598 expression had no impact on cell growth and viability as assessed by quantification of ATP levels in culture wells at different time points (Fig. 4C). HAP1 cells lacking Vigilin, SERBP1, or ZNF598 expression were poorly permissive to DENV infection as shown by the quantification of viral progeny in supernatants of infected cells (Fig. 4D), Western blot analysis of the DENV protein expression (NS3, E, and PrM)

FIG 2 Legend (Continued)

(C) Interaction network of RACK1-associated proteins identified by MS in 293T cells. Proteins were clustered into functional modules using enriched GO terms as a guideline and manual mining of literature. This panel is a representative network of *n* = 3 independent experiments showing similar results. LC-MS/MS, liquid chromatography-tandem MS.

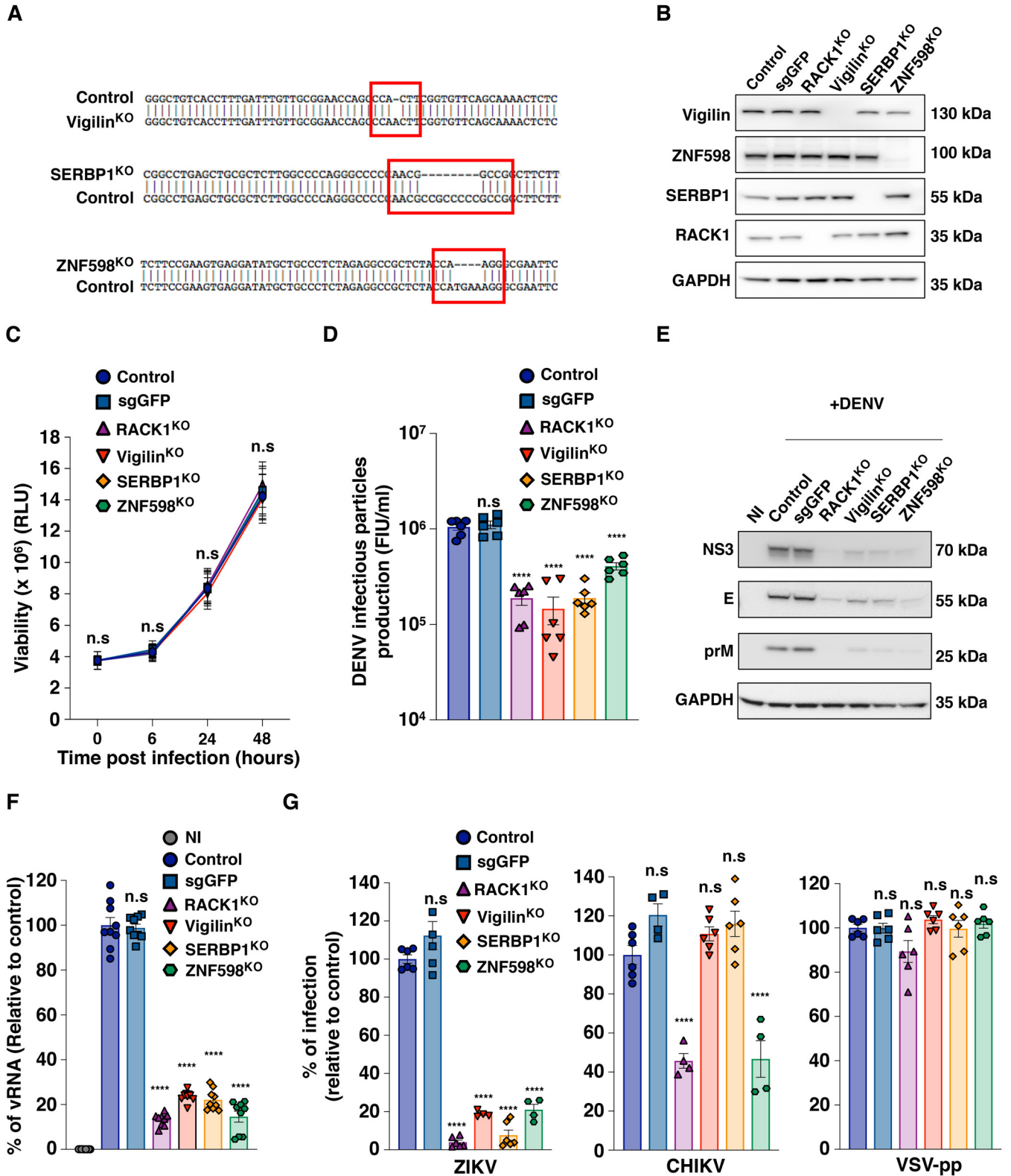


FIG 4 Impact of RACK1, Vigilin, SERBP1, and ZNF598 gene editing on infection by DENV and other enveloped viruses. (A) Sanger sequencing of *VIGILIN*, *SERBP1*, and *ZNF598* in control and Vigilin^{KO}, SERBP1^{KO}, or ZNF598^{KO} HAP1 cells, respectively. (B) Validation of Vigilin, SERBP1, and ZNF598 gene editing by Western blot analysis. Shown is a representative Western blot of three independent experiments. (C) Impact of RACK1, Vigilin, SERBP1, and ZNF598 gene editing on cell viability in HAP1 cells by cell titer glow analysis. The data shown are the means ± SEM of three independent experiments performed in duplicate. Significance was calculated using two-way ANOVA with Dunnett’s multiple-comparison test. (D to G) Impact of RACK1/Vigilin/SERBP1/ZNF598 gene editing on DENV infectious cycle. The indicated cells were infected for 48 h at MOI 1 with DENV2-16681. (D) Supernatants from infected cells were

(Continued on next page)

(Fig. 4E), and quantification of the viral RNA (Fig. 4F). Parental (control) and HAP1 cells transfected with a nonspecific single guide RNA (targeting the green fluorescent protein [GFP]) were used as negative controls (Fig. 4), while RACK1^{KO} HAP1 cells were used as positive controls (Fig. 4). We then investigated whether these phenotypes were specific to DENV2-16681 or could be observed with other flaviviruses. We found that Vigilin, SERBP1, and ZNF598 mediate infection by other DENV serotypes (data not shown), as well as by Zika virus (ZIKV), a related flavivirus (Fig. 4G). In contrast, infections by the *Alphavirus* chikungunya virus (CHIKV) or the vesicular stomatitis virus G protein (VSV-G)-pseudotyped human immunodeficiency virus (VSVpp) were unaffected in Vigilin^{KO} and SERBP1^{KO} cells (Fig. 4G). CHIKV infection but not VSVpp was significantly reduced in RACK1^{KO} and ZNF598^{KO} cells (Fig. 4G). Altogether, our data indicate that Vigilin, SERBP1, and ZNF598 are important host factors for DENV. ZNF598 is required for DENV and CHIKV infection, while Vigilin and SERBP1 are exclusively exploited by DENV and other related flaviviruses.

Vigilin and SERBP1 regulate DENV translation and replication. To determine whether Vigilin and SERBP1 impact initial vRNA translation or amplification, Vigilin^{KO} and SERBP1^{KO} cells were challenged with DENV2 *Renilla* luciferase (Luc) reporter virus (DV-R2A) through a time-course experiment to monitor the kinetic of viral infection (Fig. 5A). RACK1^{KO} cells were used as a positive control. A weak Luc activity was detected at 6 h postinfection, reflecting the initial translation of the incoming vRNA. This was followed by a marked increase in Luc activity caused by a combination of translation and replication of the viral genome (Fig. 5A). Depletion of RACK1, Vigilin, and SERBP1 had no impact on initial translation step but strongly impaired DENV translation and replication at later time points (Fig. 5A). Importantly, viral genome replication was completely restored in KO cells transduced with RACK1, SERBP1, or Vigilin cDNAs (Fig. 5A). CHIKV expressing the *Gaussia* luciferase replicated as efficiently in Vigilin or SERBP1^{KO} cells as in control cells, while its replication in RACK1^{KO} was impaired (Fig. 5B). To assess further the effect of Vigilin and SERBP1 on DENV vRNA replication, we used a *Renilla* luciferase (Rluc) reporter subgenomic replicon (sgDVR2A), which is a self-replicating DENV RNA containing a large in-frame deletion in the structural genes and represents a useful tool to exclusively monitor DENV translation and RNA amplification. Control, Vigilin^{KO}, SERBP1^{KO}, and RACK1^{KO} HAP1 cells were transfected with the *in vitro* transcribed DENVR2A subgenomic RNA, and vRNA replication was monitored over time by quantifying the Rluc activity in infected cell lysates (Fig. 5C). Depletion of RACK1, Vigilin, or SERBP1 had no impact during the early phase of DENV RNA translation. At 12 h posttransfection, the RLuc signal increased over time in control cells, while a strong reduction was observed (more than 10-fold reduction at 48 h postinfection [hpi]) in Vigilin^{KO} and SERBP1^{KO} cells (Fig. 5C). The RLuc signal was restored in Vigilin^{KO} or SERBP1^{KO} transcomplemented with their corresponding cDNAs (Fig. 5C).

Vigilin has been previously shown to mediate, in association with the host factor RBP1, the stability of DENV vRNA (47). Since SERBP1 also binds the DENV RNA (50), we reasoned that it might play a similar role. To assess this hypothesis, RACK1^{KO}, Vigilin^{KO}, or SERBP1^{KO} HAP1 cells were challenged with DENV followed by treatment with MK0608 to inhibit viral replication (47). Then, we monitored the decay of the vRNA overtime by Northern blotting analysis using a probe that targets the DENV 3'-UTR (Fig. 6). We observed that the levels of the DENV genomic RNA were similar in control,

FIG 4 Legend (Continued)

harvested, and then the titer was determined by flow cytometry on Vero cells and expressed as fluorescence-activated cell sorter infectious unit (FIU)/mL. (E) Infection was assessed by immunoblot using anti-NS3, anti-prM, and anti-E DENV MAbs. The data shown are representative of three independent experiments. (F) Levels of infection were assessed by quantification of DENV viral RNA (vRNA) by quantitative reverse transcription-PCR using NS3 primers. The data shown are the means \pm SEM of three independent experiments performed in duplicate. Significance was calculated using one-way ANOVA. (G) The indicated cells were infected with Zika virus (ZIKV) HD78 at MOI 2 (left), chikungunya virus (CHIKV) 21 at MOI 2 (middle), and vesicular stomatitis virus G protein-pseudotyped human immunodeficiency virus (VSV-pp) at MOI 2 (right). Levels of infection were determined by flow cytometry at 48 hpi. The data shown are the means \pm SEM of at least two independent experiments performed in duplicate. Significance was calculated using one-way ANOVA with Dunnett's multiple-comparison test. n.s., not significant; ****, $P < 0.0001$.

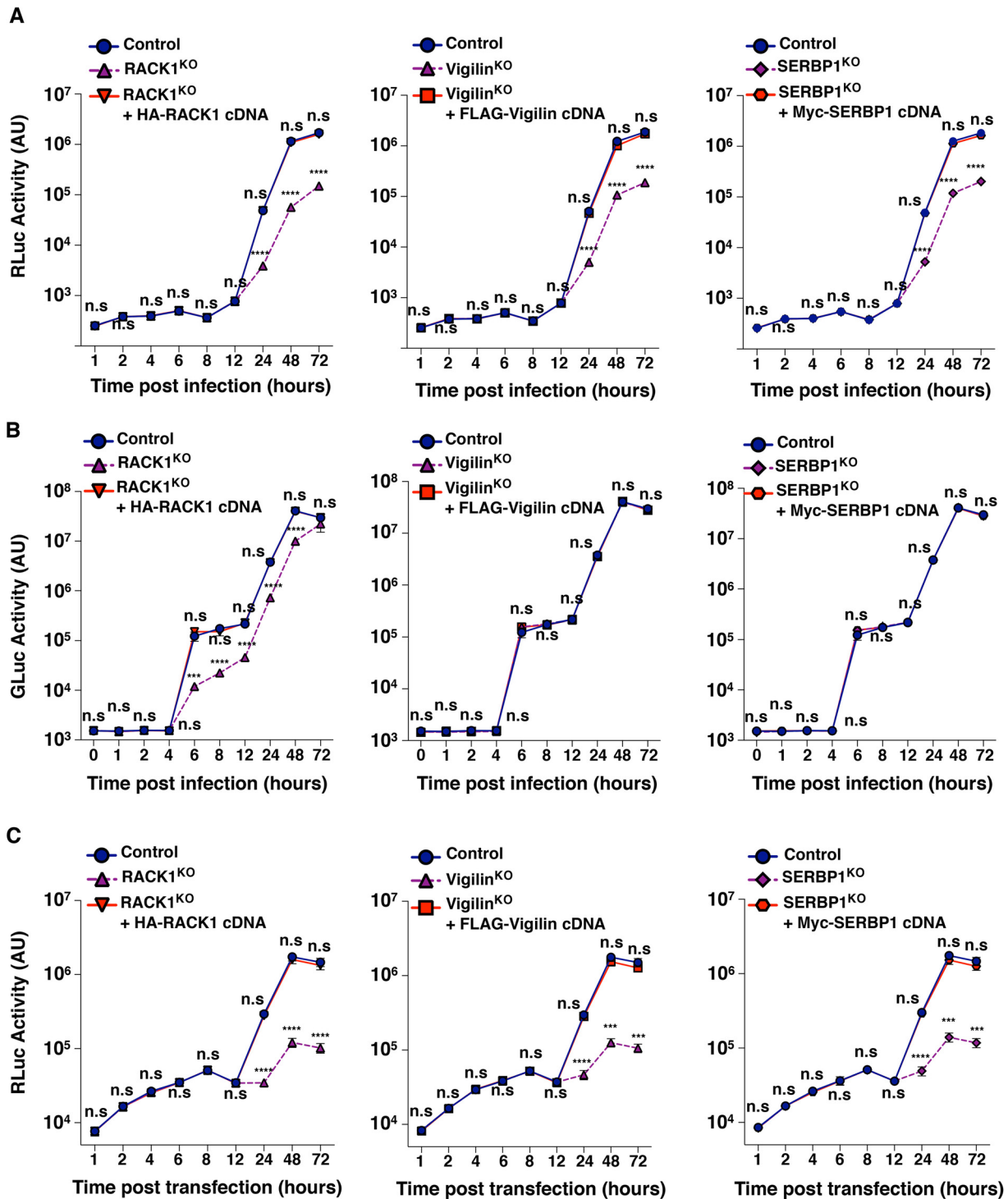
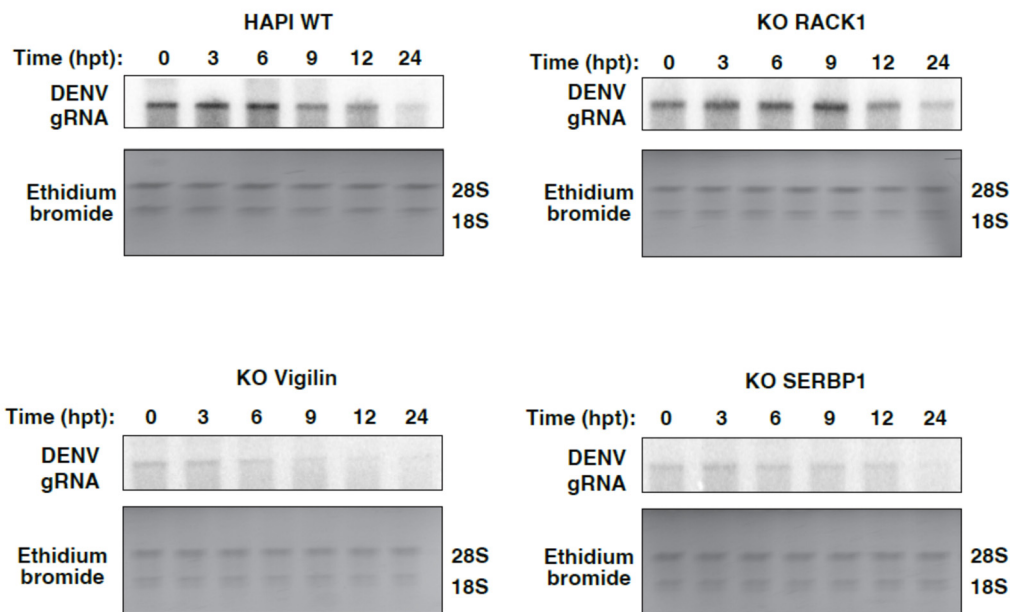


FIG 5 Vigilin and SERBP1 regulate DENV translation and replication. (A) The indicated cells were infected at MOI 1 with DENV-Luc. At the indicated time points, *Renilla* luciferase activity reflecting RNA translation (1 to 8 hpi) and replication (12 to 72 hpi) was measured. The data shown are the means \pm SEM of three independent experiments performed in triplicate. Significance was calculated using two-way ANOVA with Dunnett's multiple-comparison test. (B) The indicated cells were infected at MOI 1 with CHIKV-Luc. *Gussia* luciferase activity was monitored at the indicated time points. The data shown are the means \pm SEM of three independent experiments performed in triplicate. Significance was calculated using two-way ANOVA with Dunnett's multiple-comparison test. (C) Impact of RACK1/Vigilin/SERBP1 KO on DENV life cycle in HAP1 cells transfected with a DENV replicon RNA expressing *Renilla* luciferase. *Renilla* luciferase activity was monitored at the indicated time point. The data shown are the means \pm SEM of three independent experiments performed in triplicate. Significance was calculated using two-way ANOVA with Dunnett's multiple-comparison test. n.s., not significant; ****, $P < 0.0001$; AU, arbitrary units; Gluc, *Gussia* luciferase; RLuc, *Renilla* luciferase.

A



B

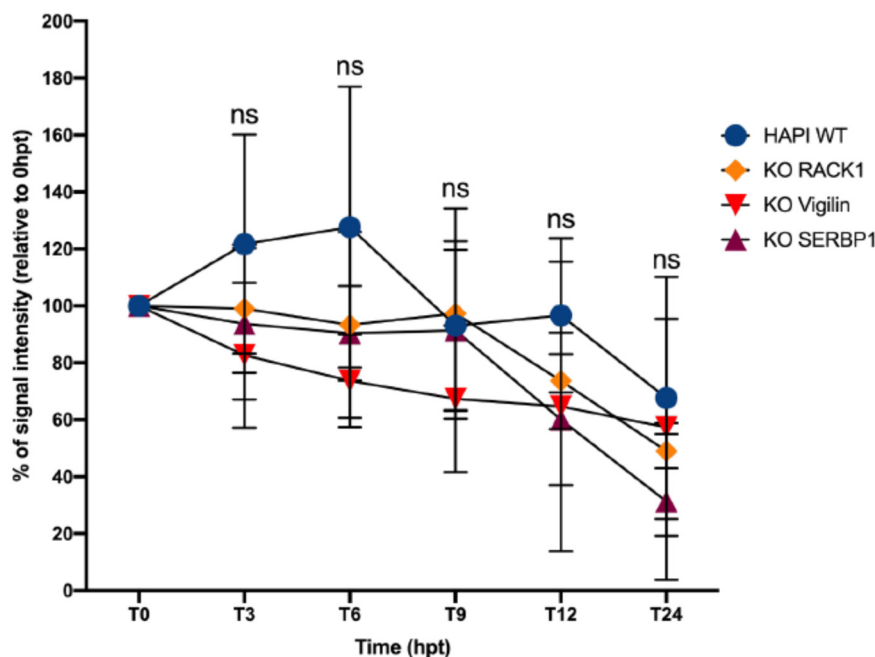


FIG 6 Northern blot analysis of the impact of RACK1, Vigilin, and SERBP1 knockout on DENV genomic RNA (gRNA) stability. (A) Indicated cells were infected at an MOI of 1 with DENV2-16681. Total RNA was extracted 48 h.p.i. at the indicated time after treatment with MK0608 replication inhibitor. The data shown are the means \pm SEM of three independent experiments performed in triplicate. (B) vRNA stability is expressed as a percentage relative to the signal monitored at time point 0 h after MK0608 treatment. Ethidium bromide serves as a loading control, showing 28S and 18S rRNA. Statistics were performed using two-way ANOVA. hpt, h posttransfection; ns, nonsignificant.

RACK1^{KO}, and SERBP1^{KO} HAPI cells up to 24 h after MK0608 treatment (Fig. 6). Surprisingly, a lack of Vigilin expression had a very mild effect on DENV RNA stability (Fig. 6). Together, these results show that RACK1, Vigilin, and SERBP1 promote viral replication without a major impact on the stability of DENV vRNA.

Vigilin and SERBP1 interactions with RACK1 are important for DENV infection.

Scp160p and Asc1p, the yeast homologs of Vigilin and RACK1, respectively, have

been shown to interact each other (24). This interaction is thought to promote translation of specific mRNAs linked to Scp160p by mediating their association with polyosomes (24). Because Vigilin is very well-conserved among different species, a similar interaction with RACK1 might occur in mammalian cells. Having established that Vigilin and SERBP1 do not have a major influence on the stability of the vRNA, we hypothesized that their proviral effect might be linked to their interaction with RACK1. Previous studies showed that Scp160p interacts with Asc1p via the KH 13 and 14 domains located in its C-terminal region (24, 52), while SERBP1 interacts directly with RACK1 through a motif (amino acids [aa] 354 to 474) that contains the RGG domain (48) (Fig. 7A). On the basis of these observations, we generated the corresponding deletion mutants of FLAG-tagged Vigilin (FLAG-Vigilin Mut) and Myc-tagged SERBP1 (Myc-SERBP1 Mut) (Fig. 7A) and tested their ability to interact with RACK1 (Fig. 7B). Pulldown experiments showed that RACK1 binds both WT FLAG Vigilin or WT Myc SERBP1 ectopically expressed in HEK-293T cells (Fig. 7B). In contrast, RACK1 failed to associate with mutant forms of Vigilin and SERBP1 (Fig. 7B). We next assessed the ability of the mutant forms to interact with DENV vRNA by performing an RNA immunoprecipitation (IP) assay after UV irradiation (Fig. 7C). For both RNA-binding proteins, the WT and mutant forms were able to specifically enrich the vRNA (at least 10-fold more than actin enrichment). Furthermore, we did not observe any significant differences in vRNA enrichment between the mutant and WT forms of the RBPs. These data demonstrate that Vigilin Mut and SERBP1 Mut bind the DENV vRNA to the same extent as their WT counterparts.

Finally, we investigated whether Vigilin and SERBP1 binding to RACK1 impacts DENV infection. For this, we stably expressed Mut Vigilin or Mut SERBP1 in Vigilin^{KO} or SERBP1^{KO} cells, respectively (Fig. 8A). Infection studies showed that expression of Mut Vigilin or Mut SERBP1 in Vigilin^{KO} or SERBP1^{KO} cells did not restore DENV2-16681 infection in contrast to their WT counterparts (Fig. 8B). Together, these data indicate that Vigilin and SERBP1 interaction with RACK1 is important for DENV infection.

Conclusions. Our results provide new insights into the molecular mechanisms of DENV replication. We performed the first RACK1 interactome in human cells and identified Vigilin and SERBP1 as host factors for DENV infection. Both are RNA-binding proteins that interact with the DENV RNA and regulate viral replication. Importantly, our data suggest that the interaction of Vigilin and SERBP1 with RACK1 are important for DENV infection. The proviral function of RACK1 depends on its association with the 40S ribosomal subunit. Furthermore, mutants of SERBP1 or Vigilin that lost their ability to interact with RACK1 were unable to support infection. We propose a model in which RACK1 acts as a binding platform at the surface of the 40S ribosomal subunit to recruit Vigilin and SERBP1, which may therefore function as linkers between the viral RNA and the translation machinery to facilitate DENV infection. Strategies that interfere with RACK1-ribosome association or disturb the RACK1-Vigilin-SERBP1 complex may represent new ways to combat DENV-induced disease.

MATERIALS AND METHODS

Cell lines. HAP1 cells (Horizon Discovery) and HAP1 RACK1^{KO} (provided by Gabriele Fuchs, University at Albany) were cultured in Iscove's modified Dulbecco's medium (IMDM) supplemented with 10% fetal bovine serum (FBS), 1% penicillin-streptomycin, 1% GlutaMAX, and 25 mM HEPES. HEK293T (ATCC), Vero E6 (ATCC), BHK-21 (ATCC), and HeLa (ATCC) cells were cultured in Dulbecco's modified Eagle's medium (DMEM) supplemented with 10% FBS, 1% penicillin-streptomycin, 1% GlutaMAX, and 25 mM HEPES. Fibroblast BJ-5ta cells (ATCC) were cultured according to the manufacturer's instructions. A final concentration of 50 μ M MK0608 was used in this study. All of the cell lines were cultured at 37°C and 5% CO₂.

Virus strains and replicons. DENV1-KDH0026A (gift from L. Lambrechts, Pasteur Institute, Paris, France), DENV2-16681 (Thailand/16681/84), DENV4 (H241), and ZIKV HD78788 were propagated in mosquito AP61 cell monolayers with limited cell passages. DENV2 Rluc reporter virus (DVR2A) was provided by Ralf Bartenschlager (University of Heidelberg). The CHIKV Luc reporter virus was described previously (53). To generate infectious virus, capped viral RNAs were generated from the NotI-linearized plasmids using a mMessage mMachine T7 transcription kit (Thermo Fisher Scientific) according to the manufacturer's instructions. RNAs were purified (see RNA IP protocol), resuspended in DNase/RNase-free water, aliquoted, and stored at -80°C until used. 30 μ g of purified RNAs were transfected in BHK21 cells using Lipofectamine 3000 reagent. Supernatants were collected 72 h later and used for viral propagation on

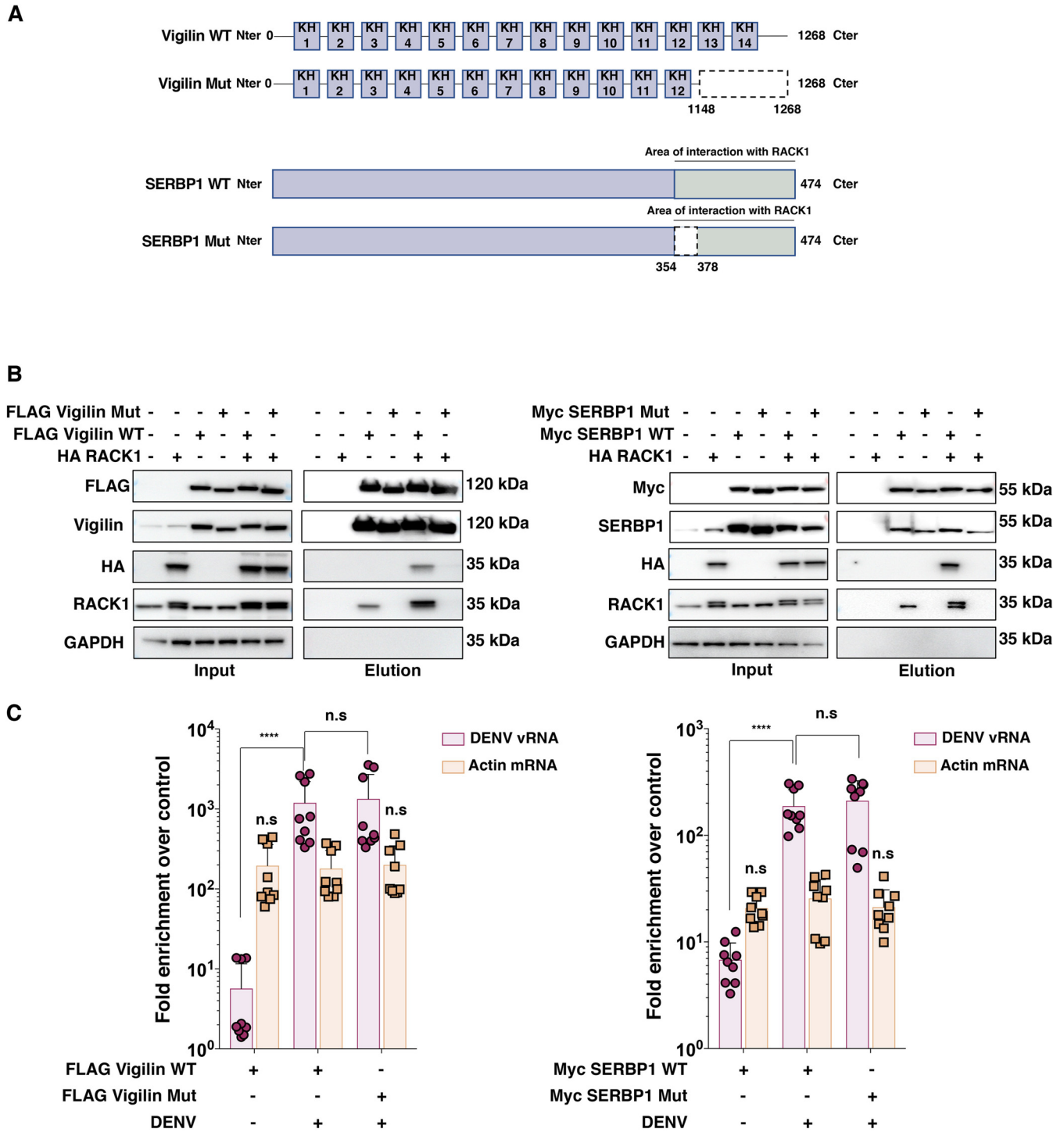


FIG 7 Characterization of Vigilin and SERBP1 mutants (Mut) deficient for RACK1 binding. (A) Schematic representations of Vigilin mutant (upper diagram) and SERBP1 mutant (lower diagram) constructs. (B) Evaluation of FLAG-Vigilin mutant (left) or Myc-SERBP1 mutant (right) interaction with RACK1. Cell extracts from 293T expressing the WT or mutated forms of Vigilin and SERBP1 were subjected to affinity purification using anti-FLAG- or -Myc-coated beads, respectively. Input and eluates were resolved by SDS-PAGE, and interacting proteins were revealed by Western blotting using corresponding antibodies. Shown is a representative Western blot of three independent experiments. (C) Analysis of Vigilin (WT and Mut) and SERBP1 (WT and Mut) interactions with the DENV RNA by RNA immunoprecipitation assay (RIP). The cells were infected at MOI 1 by DENV2-16681 and harvested 48 hpi. Tagged proteins were immunoprecipitated after UV cross-link at 254 nm using anti-FLAG- or -Myc-coated beads. The enrichment of DENV RNA or Actin RNA over the negative-control condition were determined by quantitative reverse transcription-PCR using specific primers and quantified using the $\Delta\Delta C_t$ method. The data shown are the means \pm SEM of three independent experiments performed in triplicate. Significance was calculated using a two-way ANOVA with Dunnett's multiple-comparison test. Cter, C terminus; Nter, N terminus; n.s, not significant; ****, $P < 0.0001$.

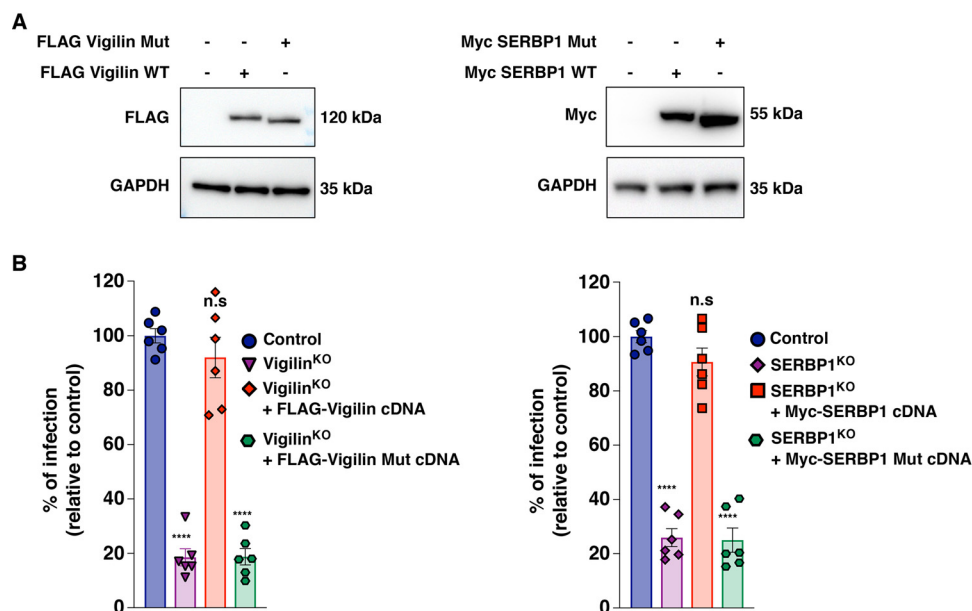


FIG 8 Vigilin and SERBP1 interaction with RACK1 is important in DENV infection. (A) Stable expression of Vigilin WT or Mut and SERBP1 WT or Mut in Vigilin^{KO} or SERBP1^{KO} HAP1 cells, respectively. Western blot analysis of Vigilin or SERBP1 expression is shown. The data shown are representative of three independent experiments. (B) The indicated cells were infected at MOI 1 with DENV2-16681. Levels of infection were determined by flow cytometry at 48 hpi using the 2H2 MAb. The data shown are the means \pm SEM of three technically independent experiments performed in duplicate. Significance was calculated using one-way ANOVA with Dunnett's multiple-comparison test. n.s, not significant; ****, $P < 0.0001$.

Vero E6 cells. For all of the viral stocks used in flow cytometry experiments, the viruses were purified through a 20% sucrose cushion by ultracentrifugation at $80,000 \times g$ for 2 h at 4°C. The pellets were resuspended in HNE1X pH 7.4 (5 mM HEPES, 150 mM NaCl, 0.1 mM EDTA), aliquoted, and stored at -80°C. Viral stock titers were determined on Vero E6 cells by plaque-forming assay and were expressed as PFU/mL. Virus stocks were also determined by flow cytometry as described (54). Vero E6 cells were incubated 1 h with 100 μ L of 10-fold serial dilutions of viral stocks. The inoculum was then replaced with 500 μ L of culture medium, and the percentage of infected cells was quantified by flow cytometry using the 2H2 anti-PrM monoclonal antibody (MAb) at 8 h after infection. Viral titers were calculated and expressed as the number of fluorescence-activated cell sorter infectious units (FIU)/mL: titer = (average percentage of infection) \times (number of cells in well) \times (dilution factor)/(mL of inoculum added to cells).

To establish a DENV replicon plasmid, based on the infectious DENV2-16681 cDNA clone, the region encoding the structural proteins was mostly deleted and replaced by a cassette encoding ubiquitin-*Renilla* luciferase-foot-and-mouth disease virus (FMDV) 2A. DENV replicon RNA was generated as previously described (12). Infection or replication was determined by measuring the luciferase activity using TriStar LB942 microplate reader (Berthold Technologies). Red fluorescent protein (RFP)-expressing lentiviral vector pseudotyped with vesicular stomatitis virus glycoprotein G (VSV-G) were generated by transfecting HEK293FT cells with pNL4.3 Luc RFP Δ Env, psPAX2, and pVSV-G (4:3:1 ratio) using Lipofectamine 3000. The supernatants were harvested 48 h after transfection, cleared by centrifugation, filtered, and frozen at -80°C.

Polysome profiling. A total of 2×10^8 of indicated cells were incubated with 100 μ g/mL of cycloheximide (CHX) for 10 min at 37°C and washed twice with cold phosphate-buffered saline (PBS) + 100 μ g/mL CHX. The cells were pelleted by centrifugation at 4°C at $300 \times g$ for 10 min and washed once with cold PBS + 100 μ g/mL CHX. The pellet was resuspended in 2 mL lysis buffer (10 mM Tris-HCl, pH 7.5, 100 mM KCl, 10 mM magnesium acetate, 1% Triton X-100, 2 mM dithiothreitol [DTT]) containing 100 μ g/mL CHX. The cells were pulverized by adding glass beads and vortexed for 5 min at 4°C. Cells debris were removed by centrifugation at 4°C at $3,000 \times rpm$ for 10 min, and the supernatant was transferred to a 2 mL cryovial. The determination of polysome concentration was done by spectrophotometric estimation, based on the fact that ribosomes are ribonucleoprotein particles. Supernatant was quickly flash-frozen in liquid nitrogen and stored in a -80°C freezer. The supernatant was loaded on a 10 to 50% sucrose gradient (31% sucrose, 50 mM Tris-acetate, pH 7.6, 50 mM NH₄Cl, 12 mM MgCl₂, 1 mM DTT) and spun for 3 h at 39,000 rpm at 4°C in an SW41 swing-out rotor. The gradient was fractionated by hand and analyzed by immunoblotting.

Mass spectrometry analysis. HAP1 cells (5×10^8), expressing either the WT or the HA-tagged RACK1 proteins, were lysed in Pierce IP lysis buffer (Thermo Scientific) in the presence of Halt protease inhibitor cocktail (Thermo Scientific) for 30 min at 4°C and then cleared by centrifugation for 30 min at $6,000 \times g$. The supernatants were incubated overnight at 4°C with anti-HA magnetic beads. The beads

were washed three times with B015 buffer (20 mM Tris-HCl, pH 7.4, 150 mM NaCl, 5 mM MgCl₂, 10% glycerol, 0.5 mM EDTA, 0.05% Triton, 0.1% Tween 20), and the immune complexes were eluted twice with HA peptide (400 mg/mL) for 30 min at room temperature (RT). The eluates were concentrated on a Pierce concentrator (PES 10K) and stored at -20°C until used. A total of three coaffinity purifications and MS analysis experiments were performed with the HA-tagged RACK1 protein or the untagged RACK1 protein as a control in 293T cells. The samples were analyzed at Taplin Biological Mass Spectrometry Facility (Harvard Medical School). Briefly, concentrated eluates issued from immunopurification of endogenous and RACK1-HA-tagged protein were separated on 10% Tris-glycine SDS-PAGE gels (Invitrogen) and stained with Imperial Protein Stain (Thermo Fisher). Individual regions of the gel were cut into 1-mm² pieces and subjected to a modified in-gel trypsin digestion procedure (55). The peptides were desalted and subjected to a nanoscale reverse-phase high-performance liquid chromatography (HPLC) (56). Eluted peptides were then subjected to electrospray ionization and then tandem mass spectrometry (MS/MS) analysis into an LTQ Orbitrap Velos Pro ion-trap mass spectrometer (Thermo Fisher Scientific, Waltham, MA). The peptides were detected, isolated, and fragmented to produce a tandem mass spectrum of specific fragment ions for each peptide. The peptide sequences were determined by matching protein databases with the acquired fragmentation pattern by the Sequest software program (Thermo Fisher Scientific, Waltham, MA) (57). All databases include a reversed version of all the sequences, and the data were filtered to less than 2% peptide false discovery rate.

Network analysis. The AP-MS data set was analyzed with SAINTexpress and MIST software (37). Of the 1,671 proteins selected in our pipeline, 193 of 1,671 showed a probability score greater than 0.80 with SAINTexpress, and 135 of 193 showed an average peptide count greater than 10. This list of 135 host proteins was analyzed with DAVID 6.8 to identify statistical enrichments for specific GO terms from the cellular component (CC) annotation (38, 39). The interaction network was built using Cytoscape 3.4.0 (40), and the proteins were clustered into functional modules using enriched GO terms as a guideline and manual curation of literature.

Small interfering RNA (siRNA) screen assay. An arrayed ON-TARGETplus SMARTpool siRNA library targeting 49 of 135 proteins of our RACK1 network, which had an average peptide count great than 28, was purchased from Horizon Discovery. To this end, HeLa or 293T cells were transfected with a 30 nM final concentration of siRNA using the Lipofectamine RNAiMax (Life Technologies). 48 h posttransfection, the cells were infected with DENV2-16681 at MOI 5. Infection was quantified 48 h postinfection by flow cytometry and viability by CellTiter-Glo 2.0 assay (Promega). Two siRNA controls were included in the screen: a nontargeting siRNA used as a reference (siNT) and a siRNA targeting RACK1 (siRACK1) as a positive control for host-dependency factors (HDFs) (12). HDFs were defined as factors whose inhibition in both cell types decreases infection by at least 50% compared to siNT and viability by at most 20% of the siNT.

Gene editing and transcomplementation experiments. Single guide RNA (sgRNA) targeting Vigilin, SERBP1, and ZNF598 were designed using the CRISPOR software (58). Sequences for all the sgRNAs are listed in Table 1. The sgRNAs were cloned into the plasmid lentiCRISPR v2 (Addgene) according to the recommendations provided by the members of the Zhang's laboratory (Broad Institute, Cambridge, MA). HAP1 cells were transiently transfected with the plasmid expressing sgRNAs and selected with puromycin until all mock-transfected cells died. Clonal cell lines were isolated by limiting dilution and assessed by DNA sequencing and immunoblot for gene editing. The human HA-RACK1 WT and HA-RACK1 DE mutant plasmids were provided by Catherine Schuster (University of Strasbourg), the FLAG-tagged Vigilin cDNA was purchased from Genscript (clone OHu17734), and the Myc-tagged SERBP1 cDNA was purchased from Genscript (clone OHu26811C). After PCR, amplification products were cloned into a SpeI-NotI-digested (RACK1), NotI-XhoI-digested (Vigilin), or EcoRI-BamHI-digested (SERBP1) pLVX-IRES-ZsGreen1 vector. SERBP1 mutant and Vigilin mutant were obtained using the Q5 site-directed mutagenesis kit (E0554) (NEB) with deletion primers using the WT cDNA in pLVX as the template. All of the primers are listed in Table 1. Lentivirus-like particles for transduction were prepared in 293T cells by cotransfecting the plasmid of interest with psPAX2 (from N. Manel's lab, Curie Institute, Paris, France) and pCMV-VSV-G at a ratio of 4:3:1 with Lipofectamine 3000 (Thermo Fisher Scientific). The supernatants were collected 48 h after transfection, centrifuged (750 × *g*, 10 min), filtered using a 0.45-μm filter, and purified through a 20% sucrose cushion by ultracentrifugation (80,000 × *g* for 2 h at 4°C). The pellets were resuspended in HNE1X, pH 7.4, aliquoted, and stored at -80°C. Cells of interest were transduced by spinoculation (750 × *g* for 2 h at 32°C) and sorted for GFP-positive cells by flow cytometry if necessary.

Flow cytometry analysis. The indicated cells were plated in 24-well plates and infected. At indicated times, the cells were trypsinized and fixed with 2% paraformaldehyde (PFA) diluted in PBS for 15 min at room temperature. The cells were incubated for 1 h at 4°C with 1 μg/mL of 3E4 anti-E2 monoclonal antibody (CHIKV), 2H2 anti-prM monoclonal antibody (MAB) (DENV), or the anti-E protein MAB 4G2 (ZIKV). Antibodies were diluted in permeabilization flow cytometry buffer (PBS supplemented with 5% FBS, 0.5% saponin, 0.1% sodium azide). After washing, the cells were incubated with 1 μg/mL of Alexa Fluor 488- or 647-conjugated goat anti-mouse IgG diluted in permeabilization flow cytometry buffer for 30 min at 4°C. Acquisition was performed with an Attune NxT flow cytometer (Thermo Fisher Scientific), and the data were analyzed by FlowJo software (TreeStar).

Infectious virus yield assay. To assess the release of infectious particles during infection, the indicated cells were inoculated for 3 h with DENV2-16681, washed once with PBS, and maintained in the culture medium for 48 h. At the indicated time points, the supernatants were collected and kept at -80°C. Vero E6 cells were incubated with 3-fold serial dilutions of supernatant for 24 h, and prM expression was quantified by flow cytometry as previously described (54).

TABLE 1 Antibodies and reagents^a

Reagent or resource	Source or sequence	Identifier
Antibodies		
Mouse anti-RACK1 (B-3)	Santa Cruz Biotechnology	sc-17754
Rabbit anti-HA tag (C29F4)	Cell Signaling	3724S
Mouse anti- β -tubulin (D-10)	Santa Cruz Biotechnology	sc-5274
Rabbit anti-Vigilin	Bethyl	A303-971A
Mouse anti-Vigilin (H-3)	Santa Cruz Biotechnology	sc-271523
Rabbit anti-ZNF598	Bethyl	A305-108A
Mouse anti-SERBP1 (1B9)	Santa Cruz Biotechnology	sc-100800
Rabbit anti-RPS3	Bethyl	A303-841A
Mouse anti-GAPDH (0411)	Santa Cruz Biotechnology	sc-47724
Mouse anti-dengue virus NS3 protein antibody	GeneTex	GTX629477
Rabbit anti-dengue virus envelope protein antibody	GeneTex	GTX127277
Rabbit anti-dengue virus prM protein antibody	GeneTex	GTX128093
Mouse anti-FLAG (M2)	Sigma-Aldrich	F1804
Mouse anti-Myc tag (9B11)	Cell Signaling	2276S
Polyclonal rabbit anti-mouse immunoglobulins/HRP	Agilent Technologies	P0260
Peroxidase AffiniPure donkey anti-rabbit IgG (H + L)	Jackson ImmunoResearch	711-035-152
Chemicals and reagents		
DMEM	Gibco	12440-053
IMDM	Gibco	41966-029
Paraformaldehyde (32%) aqueous solution	Electron Microscopy Sciences	15714
Lipofectamine RNAiMAX	Invitrogen	13778150
Lipofectamine 3000 transfection kit	Invitrogen	L3000-015
Halt protease and phosphatase inhibitor cocktail	Thermo Scientific	1861281
Bolt 4 to 12% Bis-Tris Plus gels	Invitrogen	NW04120BOX
Bolt 10% Bis-Tris Plus gel	Invitrogen	NW00100BOX
Tampon RIPA Pierce lysis buffer	Thermo Scientific	89900
20 \times Bolt MOPS SDS running buffer	Invitrogen	B0001
Pierce 1-Step transfer buffer	Thermo Scientific	84731
SuperSignal West Dura extended duration substrate	Thermo Scientific	34076
Maxima first-strand cDNA synthesis kit for reverse transcription-qPCR	Thermo Scientific	K1671
RNase H, recombinant	New England BioLabs	M0297S
TRIzol LS reagent	Ambion	10296010
RNeasy minikit	Qiagen	74106
Tampon RIPA Pierce lysis buffer	Thermo Scientific	87788
Q5 site-directed mutagenesis kit	NEB	E0554S
7-Deaza-2'-C-methyladenosine (MK0608, 50 μ M final concn)	Biosynth Carbosynth	ND08351
Power SYBR Green PCR master mix	Life Technologies, Inc.	4367659
Critical commercial assay		
Pierce <i>Gaussia</i> luciferase glow assay kit	Thermo Scientific	16160
<i>Renilla</i> luciferase assay system	Promega	E2810
CellTiter-Glo 2.0 assay	Promega	G9242
Protein assay reagent A	Bio-Rad	500-0113
Protein assay reagent B	Bio-Rad	500-0114
Protein assay reagent S	Bio-Rad	500-0115
gRNA for CRISPR/Cas9 KO		
Control	GAGCTGGACGGCGACGTAAA	
Vigilin	GTTTGTGCTGAACACCGAAGTGGGGGG	
SERBP1	AAGCCGGCGGGGGCGGCGTTGGG	
ZNF598	GGGGGCCGGATCCCGGACCATGG	
Plasmids		
pLentiCRISPRv2	Addgene	98290
pLentiCRISPRv2 sgRNA Vigilin	This paper	NA
pLentiCRISPRv2 sgRNA SERBP1	This paper	NA
pLentiCRISPRv2 sgRNA ZNF598	This paper	NA
pLVX-IRES-ZsGreen1	Takara	632187
pLVX-IRES-ZsGreen1 HA-RACK1 WT	This paper	NA
pLVX-IRES-ZsGreen1 HA-RACK1 D/E	This paper	NA
pLVX-IRES-ZsGreen1 FLAG-Vigilin	This paper	NA

(Continued on next page)

TABLE 1 (Continued)

Reagent or resource	Source or sequence	Identifier
pLVX-IRES-ZsGreen1 FLAG-Vigilin Mut	This paper	NA
pLVX-IRES-ZsGreen1 Myc-SERBP1	This paper	NA
pLVX-IRES-ZsGreen1 Myc-SERBP1 Mut	This paper	NA
Primers for site-directed mutagenesis		
Vigilin Mut forward	TAAGCGGCCGCGATCCC	
Vigilin Mut reverse	TTCGTCCATGATTTTGCGAATGGCTTTG	
SERBP1 Mut forward	GGTGCTGATGGGCAGTGG	
SERBP1 Mut reverse	CTCTTTTGACCCTCCTCTTTTAC	
qPCR primers		
DENV2 NS3 forward	TGTGCACACTGGAAAGAAGC	
DENV2 NS3 reverse	TGCGTAGTTGATGCCTTCAC	
Hs_GAPDH_2_SG QuantiTect primer assay	Qiagen	QT01192646

^oDMEM, Dulbecco's modified Eagle's medium; GAPDH, glyceraldehyde-3-phosphate dehydrogenase; gRNA, genomic RNA; HA, hemagglutinin; HRP, horseradish peroxidase; IMDM, Iscove's modified Dulbecco's medium; MOPS, morpholinepropanesulfonic acid; Mut, mutant; qPCR, quantitative PCR; RIPA, radio immunoprecipitation assay; sgRNA, specific gRNA.

Immunoblots. The cell pellets were lysed in Pierce IP lysis buffer (Thermo Fisher Scientific) containing Halt protease and phosphatase inhibitor cocktails (Thermo Fisher Scientific) for 30 min at 4°C. Equal amounts of protein, determined by DC protein assay (Bio-Rad), were prepared in 4× LDS sample buffer (Pierce) containing 25 mM dithiothreitol (DTT) and heated at 95°C for 5 min. The samples were separated on Bolt 4 to 12% Bis-Tris gels in Bolt morpholinepropanesulfonic acid (MOPS) SDS running buffer (Thermo Scientific), and the proteins were transferred onto a polyvinylidene difluoride (PVDF) membrane (Bio-Rad) using the Power Blotter system (Thermo Fisher Scientific). The membranes were blocked with PBS containing 0.1% Tween 20 and 5% nonfat dry milk and incubated overnight at 4°C with primary antibodies (HA 1/5,000, RACK1 1/4,000, glyceraldehyde-3-phosphate dehydrogenase [GAPDH] 1/5,000, Vigilin 1/500, SERBP1 1/2,000, NS3 DENV 1/4,000, 2H2 pRm DENV 1/4,000, E DENV 1/5,000, FLAG 1/2,000, Myc 1/1,000, tubulin 1/500, ZNF598 1/10,000, anti-mouse horseradish peroxidase [HRP] 1/5,000, anti-rabbit HRP 1/10,000). Staining was revealed with corresponding HRP-coupled secondary antibodies and developed using Super Signal West Dura extended duration substrate (Thermo Fisher Scientific) following the manufacturer's instructions. The signals were acquired with a Fusion Fx camera (VILBERT Lourmat).

Coimmunoprecipitation assay. The indicated cells were plated in 10-cm dishes (5×10^6). After 24 h, the cells were transfected with a total of 15 μ g DNA expression plasmids (7.5 μ g of each plasmid in cotransfection assays) using Lipofectamine 3000 (Thermo Fisher Scientific). After 24 h of transfection, the cells were washed once with PBS, collected, and centrifuged ($400 \times g$ for 5 min). The cell pellets were lysed in Pierce IP lysis buffer (Thermo Fisher Scientific) containing Halt protease and phosphatase inhibitor cocktails (Thermo Fisher Scientific) for 30 min at 4°C. Equal amounts of protein, determined by DC protein assay (Bio-Rad), were incubated overnight at 4°C, with either anti-FLAG magnetic beads, anti-HA magnetic beads, or anti-Myc magnetic beads. The beads were washed three times with BO15 buffer (20 mM Tris-HCl, pH 7.4, 150 mM NaCl, 5 mM MgCl₂, 10% glycerol, 0.5 mM EDTA, 0.05% Triton X-100, 0.1% Tween 20) before incubation. The retained complexes were eluted twice with either 3× FLAG peptide (200 μ g/mL, Sigma-Aldrich), HA peptide (400 μ g/mL, Roche), or cMyc peptide (200 μ g/mL, Sigma-Aldrich) for 30 min at RT. The samples were prepared and immunoblotted as described above. For input, 1% of whole-cell lysates was loaded on the gel.

RNA immunoprecipitation. Indicated cells (2×10^6) were plated in 10-cm dishes, transfected for 48 h with the corresponding plasmids using Lipofectamine 3000, and then infected with DENV2-16681 at MOI 2. The culture medium was removed 48 h postinfection, and the cells were washed twice with cold PBS. The cells transfected with an empty plasmid and infected with DENV2-16681 were used as negative control to assess the experiment background. Before UV cross-link, 10 mL of cold PBS were added on the cell (2,000 mJ/cm²). The cells were collected and spun 5 min at 4°C at 2,000 rpm. The cell pellets were lysed in 1 mL of Pierce IP lysis buffer (Thermo Fisher Scientific) containing Halt protease and phosphatase inhibitor cocktails (Thermo Fisher Scientific) + 250 U of RNasin (Promega) for 30 min at 4°C. Lysates were incubated with 250 U of turbo DNase for 30 min at 37°C, then centrifugated for 15 min at 15,000 rpm. The supernatant was then collected. The protein of interest was immunoprecipitated and eluted (see the coimmunoprecipitation assay section). 100 μ l of input and elution were incubated with 150 μ l of proteinase K buffer (117 μ l NT-2, 15 μ l SDS 10%, and 18 μ l of proteinase K) 1 h at 56°C, and then 750 μ l of TRIzol reagent was added. RNA was extracted by phenol chloroform precipitation; 0.2 mL of chloroform per 1 mL of TRIzol reagent was added. The samples were vortexed vigorously for 15 s, incubated at room temperature for 3 min, and then centrifuged at $12,000 \times g$ for 15 min at 4°C. Following centrifugation, the upper aqueous phase was transferred carefully without disturbing the interphase into fresh tube. The RNA from the aqueous phase was precipitated by mixing with 0.5 mL of isopropyl alcohol per 1 mL of TRIzol reagent used for the initial homogenization. The samples were incubated at RT for 10 min and centrifuged at $12,000 \times g$ for 10 min at 2 to 4°C. The supernatant was removed completely, and the RNA pellet was washed twice with 1 mL of 75% ethanol per 1 mL of TRIzol

reagent used for the initial homogenization. The samples were mixed by vortexing and centrifuged at $7,500 \times g$ for 5 min at 2 to 8°C. The RNA pellet was air dried for 5 to 10 min and then dissolved in RNase-free water.

RNA preparation and quantitative reverse transcription-PCR. Total RNA extraction from the indicated cells was performed using the RNeasy Plus minikit (Qiagen). RNA was quantified using a Nanodrop One (Thermo Fisher Scientific) before cDNA amplification. cDNA was prepared from 100 ng total RNA with Maxima first-strand synthesis kit (Thermo Fisher Scientific) including an additional step of RNase H treatment after reverse transcription. Quantitative PCR (qPCR) was performed using Power SYBR green PCR master Mix (Thermo Fisher Scientific) on a Light Cycler 480 (Roche). Quantification was based on the comparative threshold cycle (Ct) method, using GAPDH as endogenous reference control. For RNA immunoprecipitation assays (RIPs), cDNA amplification was performed on 2 μ l of immunoprecipitated and input RNA. To assess for vRNA and actin enrichment, the $\Delta\Delta$ Ct values were calculated as previously described (59). Briefly, we normalized each RIP fractions' Ct to the corresponding input fraction Ct average for the same qPCR assay (Δ Ct [normalized RIP]) to account for sample preparation differences. Then, we adjusted the normalized RIP fraction Ct value for the normalized WT Ct value ($\Delta\Delta$ Ct = Δ Ct[normalized RIP] - Δ Ct[normalized negative control]). Finally, we performed a linear conversion of the $\Delta\Delta$ Ct ($2^{\Delta\Delta$ Ct} [- $\Delta\Delta$ Ct]) to calculate the fold change over the negative-control condition.

Cell viability assay. Cell viability and proliferation were assessed using CellTiter-Glo 2.0 assay (Promega) according to the manufacturer's protocol. The cells (3×10^4) were plated in 48-well plates. At the indicated times, 100 μ L of CellTiter-Glo reagent were added to each well. After 10 min of incubation, 200 μ L from each well was transferred in an opaque 96-well plate (Cellstar, Greiner Bio-One), and luminescence was measured on a TriStar2 LB 942 (Berthold) with a 0.1-s integration time.

RNA stability measurement by high-molecular-weight Northern blot analysis. The indicated cells (1×10^6) were plated on a 60-mm dish and infected with DENV2-16681. At 48 h postinfection, medium was replaced by MK0608 (50 μ M final concentration) containing medium to block viral replication. At the indicated time posttreatment, the cells were washed twice with cold PBS and harvested in TRIzol (Thermo Fisher Scientific). Total RNA extraction was performed as previously described in RIP protocol. The DENV2-specific probe was obtained after PCR amplification of the 3'-UTR of the DENV2-16681 infectious clone (from 10,205 to 10,704). The probes were then labeled with [α - 32 P]dCTP using the Prime-a-gene kit (Promega). For high-molecular-weight Northern blot analysis to detect DENV2 genomic RNA, 5 μ g of total RNA were denatured for 5 min at 65°C in RNA sample buffer (32% deionized formamide, 4% formaldehyde, 1 \times MOPS, 1 μ g/ μ L ethidium bromide). Then, RNA loading buffer (50% glycerol, 1 mM EDTA, 0.4% bromophenol blue) was added. RNAs were resolved in a 1% agarose gel containing 1 \times MOPS and 3.7% formaldehyde in 1 \times MOPS buffer, before being transferred overnight on a nylon Hybond N⁺ membrane (Cytiva) in a 20 \times SSC solution (Euromedex). RNAs were UV cross-linked (120 mJ) with Stratagene Stratalinker 1800 (LabX). The membrane was blocked and hybridized overnight at 42°C using PerfectHyb Plus hybridization buffer (Sigma) with the corresponding labeled probe. The day after, the membrane was washed using 2 \times SSC, 0.1% SDS solution twice at 42°C and 0.1 \times SSC, 0.1% SDS twice at 50°C before being exposed on an imaging plate (Fujifilm) for 24 h. The plate was revealed using Typhoon FLA 7,000 (GE Healthcare). Densitometry analysis of the bands was performed using Image Quant TL 8.1 software (GE Healthcare).

Graphics and statistical analyses. The number of independent experimental replications is indicated in the legends. Graphical representation and statistical analyses of mean and standard error of the mean (SEM) were performed using Prism 8 software (GraphPad Software) as well as analysis of variance (ANOVA).

Data availability. The mass spectrometry proteomics data have been deposited in the ProteomeXchange Consortium via the PRIDE partner repository with the data set identifier PXD030765 (<https://www.ebi.ac.uk/pride/archive/projects/PXD030765>).

SUPPLEMENTAL MATERIAL

Supplemental material is available online only.

SUPPLEMENTAL FILE 1, PDF file, 0.1 MB.

ACKNOWLEDGMENTS

We thank Karim Majzoub and Alessia Zamborlini for critical readings of the manuscript and helpful discussions. We are grateful to Ralf Bartenschlager (Heidelberg University, Heidelberg, Germany), Gabriele Fuchs (University at Albany, Albany, NY), and Catherine Schuster (University of Strasbourg, Strasbourg, France) for providing us with DENV R2A reporter virus, RACK1 knockout cells, and RACK1 plasmids, respectively.

A.A. dedicates this work to the memory of Jean-Louis Virelizier (Unité d'Immunologie Virale, Institut Pasteur, Paris, France) and Renaud Mahieux (Ecole Normale Supérieure, Lyon, France), who left us during the SARS-CoV-2 epidemic.

This study was supported by Fondation pour la Recherche Médicale grant FRM-EQU202003010193, the French government's Investissement d'Avenir program, Laboratoire d'Excellence Integrative Biology of Emerging Infectious Diseases grant

ANR-10-LABX-62-IBEID, and ZIKAHOST grant ANR-15-CE15-00029. A.B. was supported by a scholarship from the French Ministry of Research.

A.B., M.-L.H., and A.A. conceived the study. A.B., M.-L.H., M.P., L.C., L.B.-M., C.D., L.M., and A.A. designed the experiments. A.B. and M.-L.H. performed the RACK1 interactome and the RNAi screen. P.-O.V. provided help in the data analysis. M.P., L.C., L.B.-M., and V.K. generated the viruses used in this study and performed infection studies. B.M.K. generated the DENV replicon and provided expertise in viral RNA production. S.P. and M.B. performed the DENV RNA stability experiments. S.G.-M. participated in the RNA IP experiments. A.B. and A.A. wrote the initial manuscript draft, and the other authors contributed to its editing in its final form.

We declare no conflict of interest.

REFERENCES

- Holbrook MR. 2017. Historical perspectives on flavivirus research. *Viruses* 9:97. <https://doi.org/10.3390/v9050097>.
- Halstead SB. 2007. Dengue. *Lancet* 370:1644–1652. [https://doi.org/10.1016/S0140-6736\(07\)61687-0](https://doi.org/10.1016/S0140-6736(07)61687-0).
- Brady OJ, Gething PW, Bhatt S, Messina JP, Brownstein JS, Hoen AG, Moyes CL, Farlow AW, Scott TW, Hay SI. 2012. Refining the global spatial limits of dengue virus transmission by evidence-based consensus. *PLoS Negl Trop Dis* 6:e1760. <https://doi.org/10.1371/journal.pntd.0001760>.
- Bhatt S, Gething PW, Brady OJ, Messina JP, Farlow AW, Moyes CL, Drake JM, Brownstein JS, Hoen AG, Sankoh O, Myers MF, George DB, Jaenisch T, Wint GRW, Simmons CP, Scott TW, Farrar JJ, Hay SI. 2013. The global distribution and burden of dengue. *Nature* 496:504–507. <https://doi.org/10.1038/nature12060>.
- Kaptein SJF, Goethals O, Kiemel D, Marchand A, Kesteleyn B, Bonfanti J-F, Bardiot D, Stoops B, Jonckers THM, Dallmeier K, Gelyukens P, Thys K, Crabbe M, Chatel-Chaix L, Münster M, Querat G, Touret F, de Lamballerie X, Rabaïsson P, Simmen P, Chaltin P, Bartenschlager R, Van Loock M, Neyts J. 2021. A pan-serotype dengue virus inhibitor targeting the NS3-NS4B interaction. *Nature* 598:504–509. <https://doi.org/10.1038/s41586-021-03990-6>.
- Hadinegoro SR, Arredondo-García JL, Capeding MR, Deseda C, Chotpitayasunondh T, Dietze R, HJ Muhammad Ismail HI, Reynales H, Limkittikul K, Rivera-Medina DM, Tran HN, Bouckennooghe A, Chansinghakul D, Cortés M, Fanouillere K, Forrat R, Frago C, Gailhardou S, Jackson N, Noriega F, Plennevaux E, Wartel TA, Zambrano B, Saville M, CYD-TDV Dengue Vaccine Working Group. 2015. Efficacy and long-term safety of a dengue vaccine in regions of endemic disease. *N Engl J Med* 373:1195–1206. <https://doi.org/10.1056/NEJMoa1506223>.
- Ferguson NM, Rodríguez-Barraquer I, Dorigatti I, Mier-y-Teran-Romero L, Laydon DJ, Cummings DAT. 2016. Benefits and risks of the Sanofi-Pasteur dengue vaccine: modeling optimal deployment. *Science* 353:1033–1036. <https://doi.org/10.1126/science.aaf9590>.
- Acosta EG, Kumar A, Bartenschlager R. 2014. Revisiting dengue virus-host cell interaction: new insights into molecular and cellular virology. *Adv Virus Res* 88:1–109. <https://doi.org/10.1016/B978-0-12-800098-4.00001-5>.
- Zeidler JD, Fernandes-Siqueira LO, Barbosa GM, Da Poian AT. 2017. Non-canonical roles of dengue virus non-structural proteins. *Viruses* 9:42. <https://doi.org/10.3390/v9030042>.
- Miller S, Krijnse-Locker J. 2008. Modification of intracellular membrane structures for virus replication. *Nat Rev Microbiol* 6:363–374. <https://doi.org/10.1038/nrmicro1890>.
- Welsch S, Miller S, Romero-Brey I, Merz A, Bleck CKE, Walther P, Fuller SD, Antony C, Krijnse-Locker J, Bartenschlager R. 2009. Composition and three-dimensional architecture of the dengue virus replication and assembly sites. *Cell Host Microbe* 5:365–375. <https://doi.org/10.1016/j.chom.2009.03.007>.
- Hafirassou ML, Meertens L, Umaña-Díaz C, Labeau A, Dejarnac O, Bonnet-Madin L, Kümmerer BM, Delaugerre C, Roingard P, Vidalain P-O, Amara A. 2017. A global interactome map of the dengue virus NS1 identifies virus restriction and dependency host factors. *Cell Rep* 21:3900–3913. <https://doi.org/10.1016/j.celrep.2017.11.094>.
- Shue B, Chiramel AI, Cerikan B, To T-H, Frölich S, Pederson SM, Kirby EN, Eyre NS, Bartenschlager RFW, Best SM, Beard MR. 2021. Genome-wide CRISPR screen identifies RACK1 as a critical host factor for flavivirus replication. *J Virol* 95:e00596-21. <https://doi.org/10.1128/JVI.00596-21>.
- Ben-Shem A, Garreau de Loubresse N, Melnikov S, Jenner L, Yusupova G, Yusupov M. 2011. The structure of the eukaryotic ribosome at 3.0 Å resolution. *Science* 334:1524–1529. <https://doi.org/10.1126/science.1212642>.
- Sengupta J, Nilsson J, Gursky R, Spahn CMT, Nissen P, Frank J. 2004. Identification of the versatile scaffold protein RACK1 on the eukaryotic ribosome by cryo-EM. *Nat Struct Mol Biol* 11:957–962. <https://doi.org/10.1038/nsmb822>.
- Xu C, Min J. 2011. Structure and function of WD40 domain proteins. *Protein Cell* 2:202–214. <https://doi.org/10.1007/s13238-011-1018-1>.
- Nielsen MH, Flygaard RK, Jenner LB. 2017. Structural analysis of ribosomal RACK1 and its role in translational control. *Cell Signal* 35:272–281. <https://doi.org/10.1016/j.cellsig.2017.01.026>.
- Adams DR, Ron D, Kiely PA. 2011. RACK1, a multifaceted scaffolding protein: structure and function. *Cell Commun Signal* 9:22. <https://doi.org/10.1186/1478-811X-9-22>.
- Gandin V, Senft D, Topisirovic I, Ronai ZA. 2013. RACK1 function in cell motility and protein synthesis. *Genes Cancer* 4:369–377. <https://doi.org/10.1177/1947601913486348>.
- Chang BY, Conroy KB, Machleder EM, Cartwright CA. 1998. RACK1, a receptor for activated C kinase and a homolog of the β subunit of G proteins, inhibits activity of Src tyrosine kinases and growth of NIH 3T3 cells. *Mol Cell Biol* 18:3245–3256. <https://doi.org/10.1128/MCB.18.6.3245>.
- Chang BY, Harte RA, Cartwright CA. 2002. RACK1: a novel substrate for the Src protein-tyrosine kinase. *Oncogene* 21:7619–7629. <https://doi.org/10.1038/sj.onc.1206002>.
- Yarwood SJ, Steele MR, Scotland G, Houslay MD, Bolger GB. 1999. The RACK1 signaling scaffold protein selectively interacts with the cAMP-specific phosphodiesterase PDE4D5 isoform. *J Biol Chem* 274:14909–14917. <https://doi.org/10.1074/jbc.274.21.14909>.
- Kiely PA, Sant A, O'Connor R. 2002. RACK1 is an insulin-like growth factor 1 (IGF-1) receptor-interacting protein that can regulate IGF-1-mediated Akt activation and protection from cell death. *J Biol Chem* 277:22581–22589. <https://doi.org/10.1074/jbc.M201758200>.
- Baum S, Bittins M, Frey S, Seedorf M. 2004. Asc1p, a WD40-domain containing adaptor protein, is required for the interaction of the RNA-binding protein Scp160p with polysomes. *Biochem J* 380:823–830. <https://doi.org/10.1042/BJ20031962>.
- Ceci M, Gaviraghi C, Gorini C, Sala LA, Offenhäuser N, Carlo Marchisio P, Biffo S. 2003. Release of eIF6 (p27BBP) from the 60S subunit allows 80S ribosome assembly. *Nature* 426:579–584. <https://doi.org/10.1038/nature02160>.
- Joshi B, Cai A-L, Keiper BD, Minich WB, Mendez R, Beach CM, Stepinski J, Stolarski R, Darzynkiewicz E, Rhoads RE. 1995. Phosphorylation of eukaryotic protein synthesis initiation factor 4E at Ser-209. *J Biol Chem* 270:14597–14603. <https://doi.org/10.1074/jbc.270.24.14597>.
- Whalen SG, Gingras A-C, Amankwa L, Mader S, Branton PE, Aebersold R, Sonenberg N. 1996. Phosphorylation of eIF-4E on serine 209 by protein kinase C is inhibited by the translational repressors, 4E-binding proteins. *J Biol Chem* 271:11831–11837. <https://doi.org/10.1074/jbc.271.20.11831>.
- Sundaramoorthy E, Leonard M, Mak R, Liao J, Fulzele A, Bennett EJ. 2017. ZNF598 and RACK1 regulate mammalian ribosome-associated quality control function by mediating regulatory 40S ribosomal ubiquitylation. *Mol Cell* 65:751–760.e4. <https://doi.org/10.1016/j.molcel.2016.12.026>.
- Long L, Deng Y, Yao F, Guan D, Feng Y, Jiang H, Li X, Hu P, Lu X, Wang H, Li J, Gao X, Xie D. 2014. Recruitment of phosphatase PP2A by RACK1 adaptor protein deactivates transcription factor IRF3 and limits type I

- interferon signaling. *Immunity* 40:515–529. <https://doi.org/10.1016/j.immuni.2014.01.015>.
30. Xie T, Chen T, Li C, Wang W, Cao L, Rao H, Yang Q, Shu H-B, Xu L-G. 2019. RACK1 attenuates RLR antiviral signaling by targeting VISA-TRAF complexes. *Biochem Biophys Res Commun* 508:667–674. <https://doi.org/10.1016/j.bbrc.2018.11.203>.
 31. Duan Y, Zhang L, Angosto-Bazarrá D, Pelegrín P, Núñez G, He Y. 2020. RACK1 mediates NLRP3 inflammasome activation by promoting NLRP3 active conformation and inflammasome assembly. *Cell Rep* 33:108405. <https://doi.org/10.1016/j.celrep.2020.108405>.
 32. Kuhn L, Majzoub K, Einhorn E, Chicher J, Pompon J, Imler J-L, Hamman P, Meignin C. 2017. Definition of a RACK1 interaction network in *Drosophila melanogaster* using SWATH-MS. *G3* 7:2249–2258. <https://doi.org/10.1534/g3.117.042564>.
 33. Majzoub K, Hafirassou ML, Meignin C, Goto A, Marzi S, Fedorova A, Verdier Y, Vinh J, Hoffmann JA, Martin F, Baumert TF, Schuster C, Imler J-L. 2014. RACK1 controls IRES-mediated translation of viruses. *Cell* 159:1086–1095. <https://doi.org/10.1016/j.cell.2014.10.041>.
 34. Jha S, Rollins MG, Fuchs G, Procter DJ, Hall EA, Cozzolino K, Sarnow P, Savas JN, Walsh D. 2017. Trans-kingdom mimicry underlies ribosome customization by a poxvirus kinase. *Nature* 546:651–655. <https://doi.org/10.1038/nature22814>.
 35. Kim HD, Kong E, Kim Y, Chang J-S, Kim J. 2017. RACK1 depletion in the ribosome induces selective translation for non-canonical autophagy. *Cell Death Dis* 8:e2800. <https://doi.org/10.1038/cddis.2017.204>.
 36. Gallo S, Ricciardi S, Manfrini N, Pesce E, Oliveto S, Calamita P, Mancino M, Maffioli E, Moro M, Crosti M, Berno V, Bombaci M, Tedeschi G, Biffo S. 2018. RACK1 specifically regulates translation through its binding to ribosomes. *Mol Cell Biol* 38:e00230-18. <https://doi.org/10.1128/MCB.00230-18>.
 37. Teo G, Liu G, Zhang J, Nesvizhskii AI, Gingras A-C, Choi H. 2014. SAINTexpress: improvements and additional features in significance analysis of interactome software. *J Proteomics* 100:37–43. <https://doi.org/10.1016/j.jprot.2013.10.023>.
 38. Huang DW, Sherman BT, Lempicki RA. 2009. Systematic and integrative analysis of large gene lists using DAVID bioinformatics resources. *Nat Protoc* 4:44–57. <https://doi.org/10.1038/nprot.2008.211>.
 39. Huang DW, Sherman BT, Lempicki RA. 2009. Bioinformatics enrichment tools: paths toward the comprehensive functional analysis of large gene lists. *Nucleic Acids Res* 37:1–13. <https://doi.org/10.1093/nar/gkn923>.
 40. Shannon P, Markiel A, Ozier O, Baliga NS, Wang JT, Ramage D, Amin N, Schwikowski B, Ideker T. 2003. Cytoscape: a software environment for integrated models of biomolecular interaction networks. *Genome Res* 13:2498–2504. <https://doi.org/10.1101/gr.1239303>.
 41. Liu Y, Shi S-L. 2021. The roles of hnRNP A2/B1 in RNA biology and disease. *Wiley Interdiscip Rev RNA* 12:e1612. <https://doi.org/10.1002/wrna.1612>.
 42. Ahn J-W, Kim S, Na W, Baek S-J, Kim J-H, Min K, Yeom J, Kwak H, Jeong S, Lee C, Kim S-Y, Choi CY. 2015. SERBP1 affects homologous recombination-mediated DNA repair by regulation of CtIP translation during S phase. *Nucleic Acids Res* 43:6321–6333. <https://doi.org/10.1093/nar/gkv592>.
 43. Cheng MH, Jansen R-P. 2017. A jack of all trades: the RNA-binding protein Vigilin. *Wiley Interdiscip Rev RNA* 8:1448.
 44. Paranjape SM, Harris E. 2007. Y box-binding protein-1 binds to the dengue virus 3'-untranslated region and mediates antiviral effects. *J Biol Chem* 282:30497–30508. <https://doi.org/10.1074/jbc.M705755200>.
 45. Brunetti JE, Sclaro LA, Castilla V. 2015. The heterogeneous nuclear ribonucleoprotein K (hnRNP K) is a host factor required for dengue virus and Junin virus multiplication. *Virus Res* 203:84–91. <https://doi.org/10.1016/j.virusres.2015.04.001>.
 46. Mobin MB, Gerstberger S, Teupser D, Campana B, Charisse K, Heim MH, Manoharan M, Tuschl T, Stoffel M. 2016. The RNA-binding protein Vigilin regulates VLDL secretion through modulation of Apob mRNA translation. *Nat Commun* 7:12848. <https://doi.org/10.1038/ncomms12848>.
 47. Ooi YS, Majzoub K, Flynn RA, Mata MA, Diep J, Li JK, van Buuren N, Rumachik N, Johnson AG, Puschnik AS, Marceau CD, Mlera L, Grabowski JM, Kirkegaard K, Bloom ME, Sarnow P, Bertozzi CR, Carette JE. 2019. An RNA-centric dissection of host complexes controlling flavivirus infection. *Nat Microbiol* 4:2369–2382. <https://doi.org/10.1038/s41564-019-0518-2>.
 48. Bolger GB. 2017. The RNA-binding protein SERBP1 interacts selectively with the signaling protein RACK1. *Cell Signal* 35:256–263. <https://doi.org/10.1016/j.cellsig.2017.03.001>.
 49. Brown A, Baird MR, Yip MC, Murray J, Shao S. 2018. Structures of translationally inactive mammalian ribosomes. *Elife* 7:e40486. <https://doi.org/10.7554/eLife.40486>.
 50. Phillips SL, Soderblom EJ, Bradrick SS, Garcia-Blanco MA. 2016. Identification of proteins bound to dengue viral RNA *in vivo* reveals new host proteins important for virus replication. *mBio* 7:e01865-15. <https://doi.org/10.1128/mBio.01865-15>.
 51. Wang G, Kowaki T, Okamoto M, Oshiumi H. 2019. Attenuation of the innate immune response against viral infection due to ZNF598-promoted binding of FAT10 to RIG-I. *Cell Rep* 28:1961–1970.e4. <https://doi.org/10.1016/j.celrep.2019.07.081>.
 52. Li A, Vargas CA, Brykailo MA, Openo KK, Corbett AH, Fridovich-Keil JL. 2004. Both KH and non-KH domain sequences are required for polyribosome association of Scp160p in yeast. *Nucleic Acids Res* 32:4768–4775. <https://doi.org/10.1093/nar/gkh812>.
 53. Meertens L, Hafirassou ML, Couderc T, Bonnet-Madin L, Kril V, Kümmerer BM, Labeau A, Brugier A, Simon-Lorieri E, Burlaud-Gaillard J, Doyen C, Pezzi L, Goupil T, Rafasse S, Vidalain P-O, Bertrand-Legout A, Gueneau L, Juntas-Morales R, Ben Yaou R, Bonne G, de Lamballerie X, Benkirane M, Roingard P, Delaugerre C, Lecuit M, Amara A. 2019. FHL1 is a major host factor for chikungunya virus infection. *Nature* 574:259–263. <https://doi.org/10.1038/s41586-019-1578-4>.
 54. Meertens L, Carnec X, Lecoïn MP, Ramdasi R, Guivel-Benhassine F, Lew E, Lemke G, Schwartz O, Amara A. 2012. The TIM and TAM families of phosphatidylserine receptors mediate dengue virus entry. *Cell Host Microbe* 12:544–557. <https://doi.org/10.1016/j.chom.2012.08.009>.
 55. Shevchenko A, Wilm M, Vorm O, Mann M. 1996. Mass spectrometric sequencing of proteins silver-stained polyacrylamide gels. *Anal Chem* 68:850–858. <https://doi.org/10.1021/ac950914h>.
 56. Peng J, Gygi SP. 2001. Proteomics: the move to mixtures. *J Mass Spectrom* 36:1083–1091. <https://doi.org/10.1002/jms.229>.
 57. Eng JK, McCormack AL, Yates JR. 1994. An approach to correlate tandem mass spectral data of peptides with amino acid sequences in a protein database. *J Am Soc Mass Spectrom* 5:976–989. [https://doi.org/10.1016/1044-0305\(94\)80016-2](https://doi.org/10.1016/1044-0305(94)80016-2).
 58. Concordet J-P, Haeussler M. 2018. CRISPOR: intuitive guide selection for CRISPR/Cas9 genome editing experiments and screens. *Nucleic Acids Res* 46:W242–W245. <https://doi.org/10.1093/nar/gky354>.
 59. Marmisolle FE, García ML, Reyes CA. 2018. RNA-binding protein immunoprecipitation as a tool to investigate plant miRNA processing interference by regulatory proteins of diverse origin. *Plant Methods* 14:9. <https://doi.org/10.1186/s13007-018-0276-9>.